John Barnard
Steven Lund
USPAS
January 12-24, 2020
San Diego, California

An application of intense beams

1. Heavy-ion fusion
   - A. Requirements
   - B. Targets for ICF
   - C. Accelerator
   - D. Drift compression
   - E. Final focus
   - F. Experiments

Inertial fusion energy (IFE) power plants of the future will consist of four parts

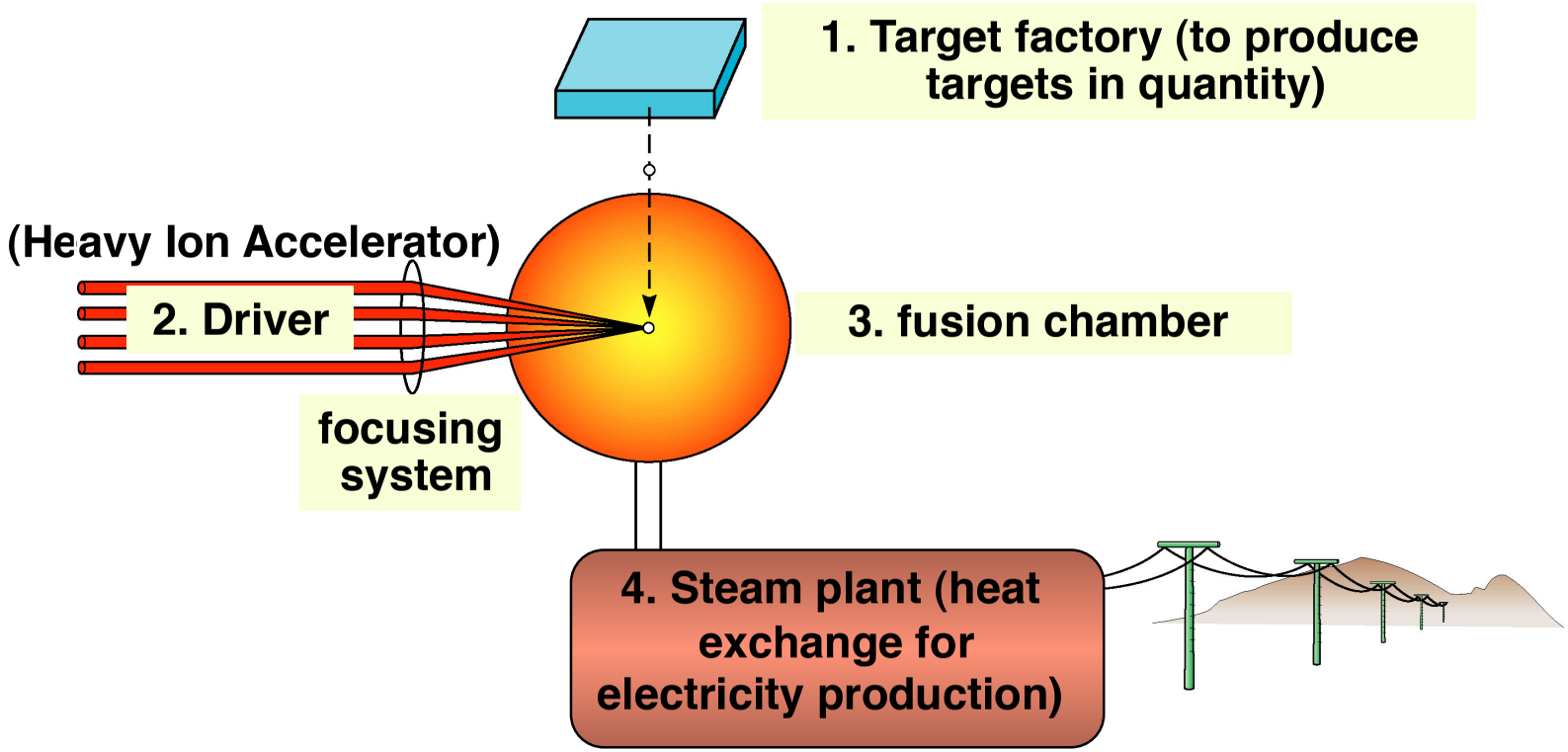

A power plant driver would fire about five targets per second to produce as much electricity as today's 1000 Megawatt power plant

Heavy Ion Fusion provides an attractive approach to long term energy production

Fusion offers an inexhaustible, long term solution solution the problem of future energy supplies free from long lived radioactive by-products and greenhouse CO_2.

Inertial Confinement Fusion (ICF) uses laser, particle beams, or electrical pulses to implode a target, raising the temperature and density of the fuel, creating the conditions necessary for the following fusion reaction:

$$D + T \rightarrow n\ (14.06\ MeV) + He^4\ (3.52\ MeV)$$

Heavy ion accelerators are a strong candidate for inertial fusion energy (IFE) power production because of:

- High efficiency
- High repetition rate
- Survivability of final lens (focusing optic can be shielded)
- Favorable target illumination geometry

Focusability at the target is key scientific issue

Conditions of beam at target are set by hohlraum and implosion physics

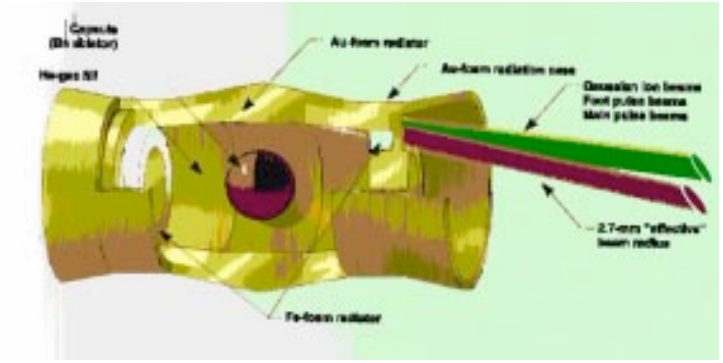

Energy in pulse: ~ 3 to 6 MJ

Duration of main pulse: ~ 8 to 10 ns

Duration of foot pulse: ~ 30 ns

Spot radius: ~ 1.5 to 3 mm

Transverse and longitudinal compression are required to meet target specifications.

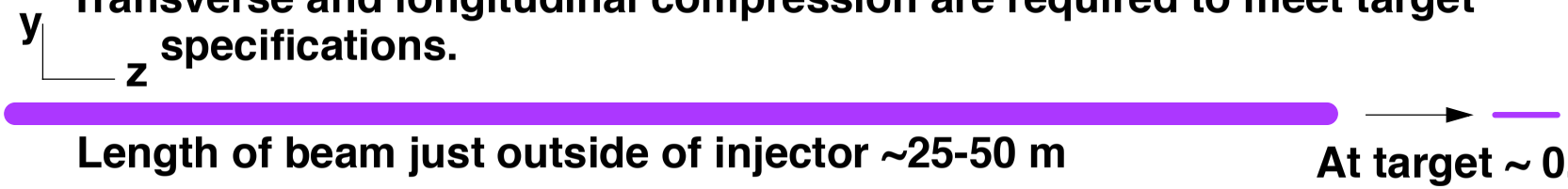

Length of beam just outside of injector ~25-50 m

At target ~ 0.5 - 1 m

Radius of beam at source ~ 1-3 cm

At target ~ 1.5-3 mm

Compression factors of 10 to 50 in both longitudinal and transverse directions are required.

6D phase space conservation ($(\varepsilon_{nx}\,\varepsilon_{ny}\,\Delta p_z\,l_b)_i < (\varepsilon_{nx}\,\varepsilon_{ny}\,\Delta p_z\,l_b)_f$) constrains designs.

National Ignition Facility (NIF) at LLNL plays a critical role in addressing IFE feasibility

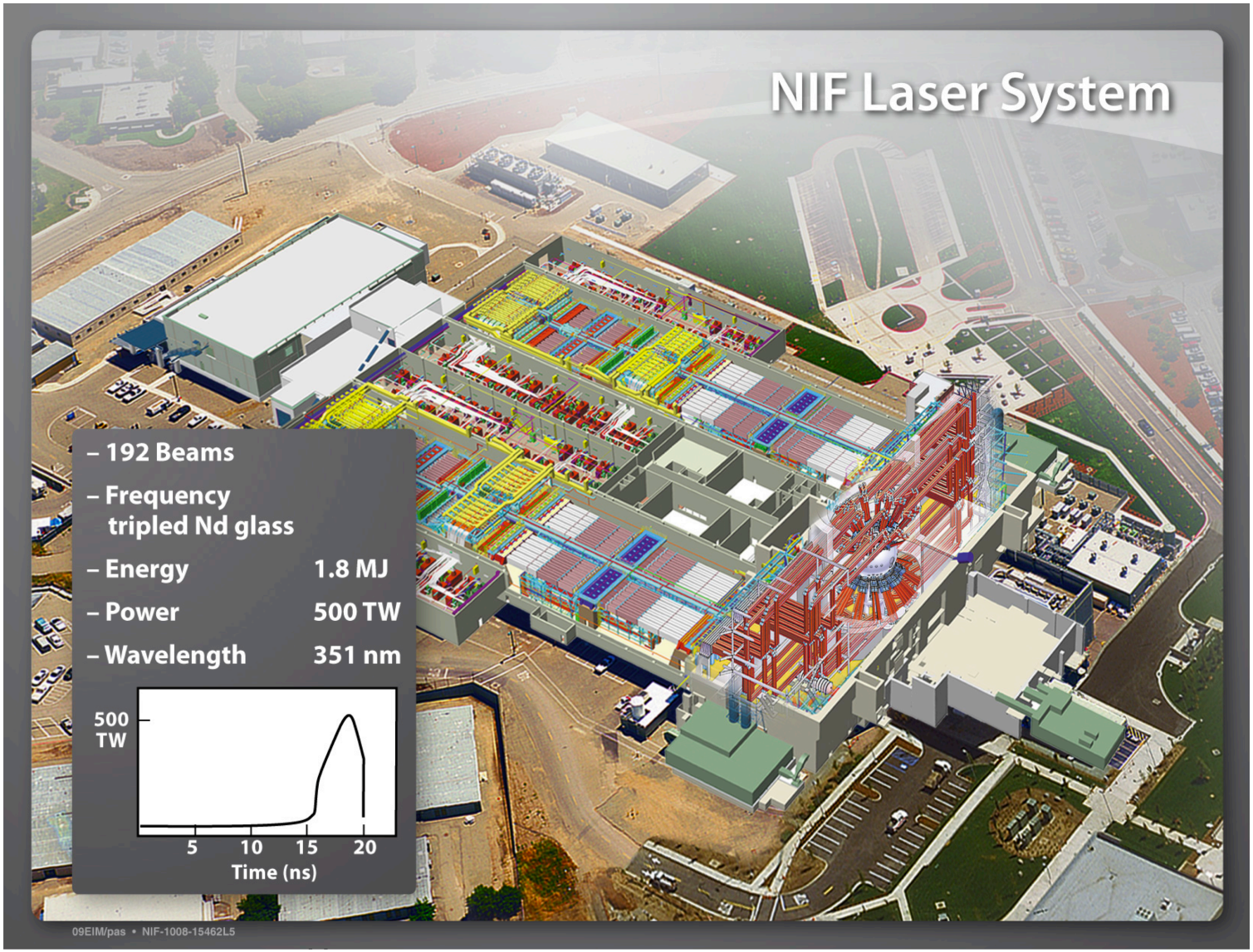

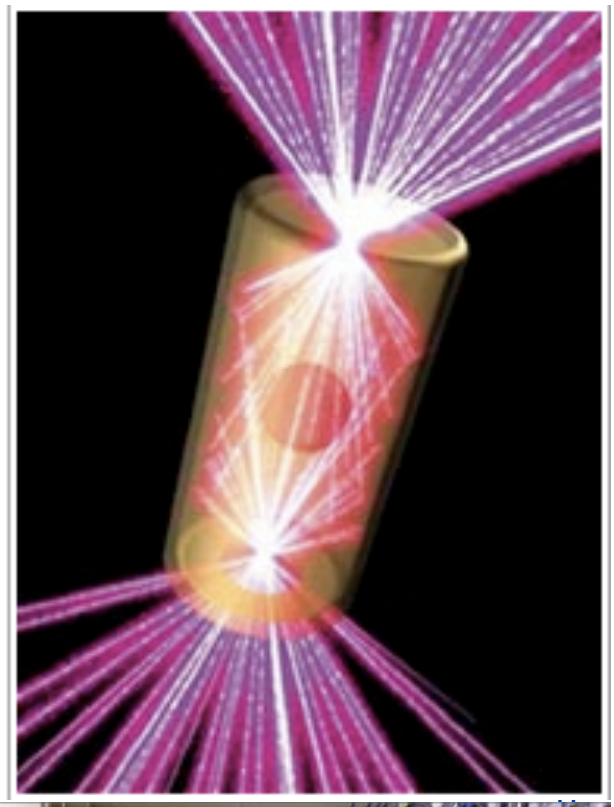

The two principal approaches to ICF are direct drive and indirect drive

Two types of targets:

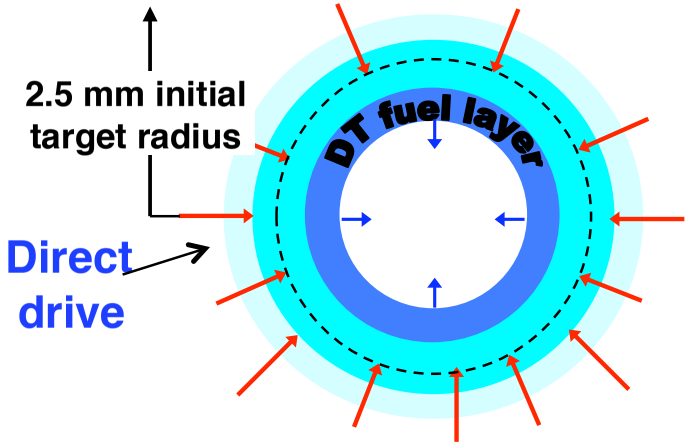

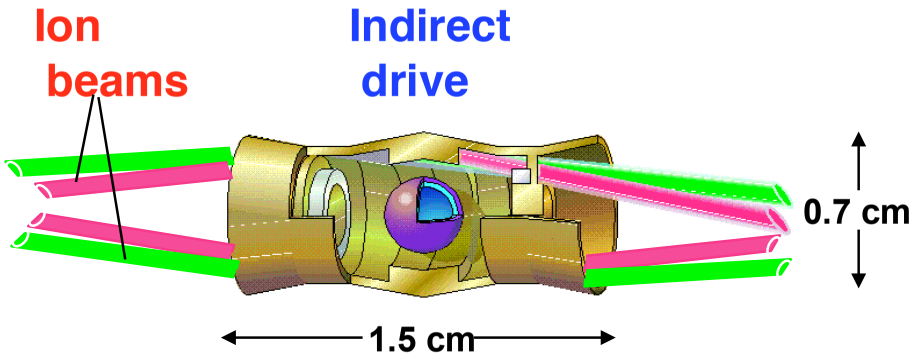

Direct drive advantages:

Higher coupling efficiency with potential for higher gain

Indirect drive advantages:

Relaxed beam uniformity (reduced hydro instability)

SIgnificant commonality for lasers and ion beams

Significant simplification of chamber geometry

From M. Rosen, American Physical Society Presentation, October 2014:

We think 3 major issues caused the degraded performance of the NIC point design ("Low foot", 4 shock CH capsule)

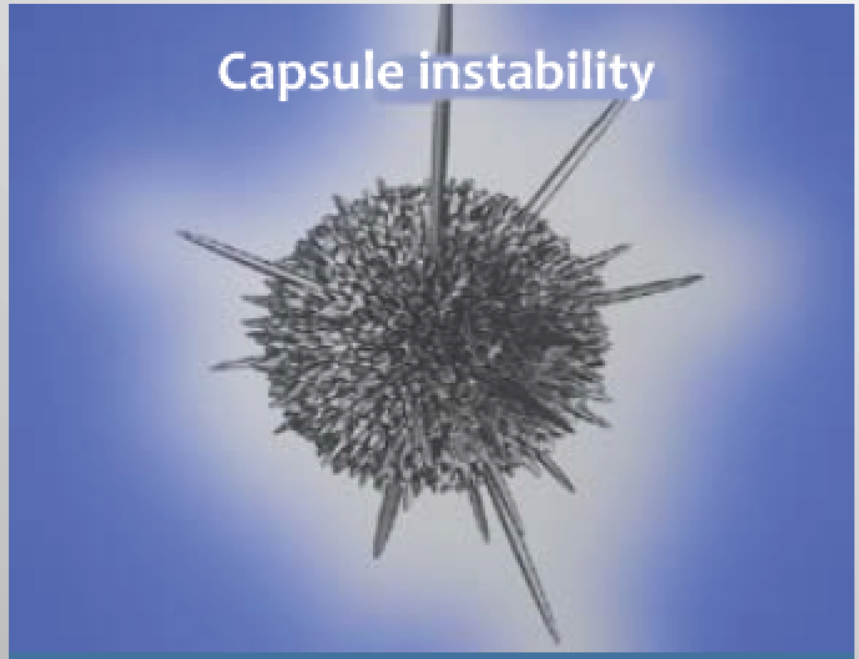

Growth x Surface seeds is too large leading to mix at lower velocity than predicted

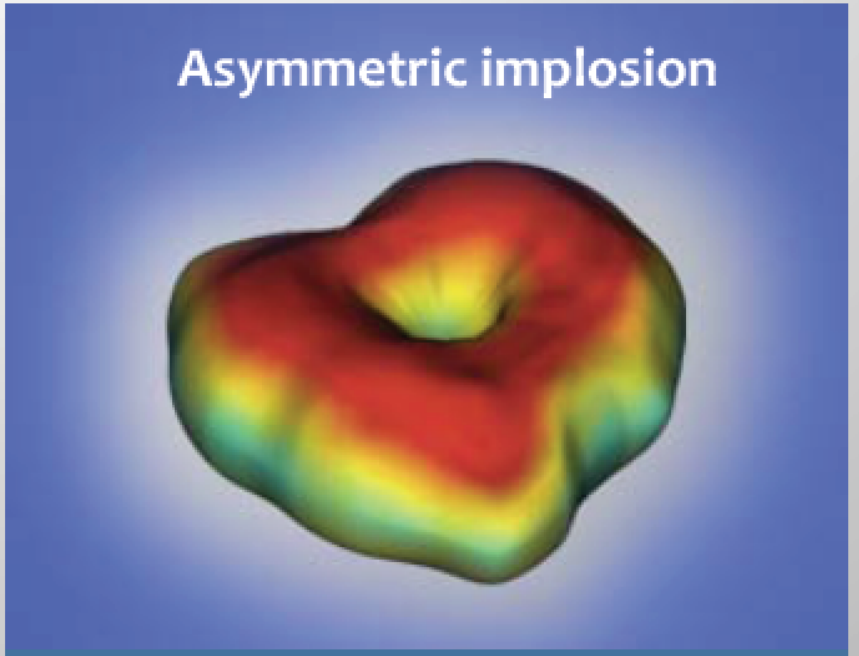

X-ray push on the capsule is not symmetric enough resulting in loss of efficiency at stagnation

The hohlraums were complicated by Raman (SRS) on the inners: This then required CBET & each affects the other. Unexplained "deficits" in drive, and hard to calculate symmetry ensued. SRS also made hot electrons, which may have affected performance.

From M. Rosen, American Physical Society Presentation, October 2014:

Current "traffic report" of the road to indirect drive ignition

- **Hydrodynamic Instabilities:** **2012:** When pushed to higher velocity, the Pt. Design hit a roadblock: **Mix** of CH ablator into the hot spot, & severely degraded performance
  - **2014:** Less stressing, more stable, CH implosions successfully pushed to higher velocity
    - Yield improvements of > 10x, and significant self heating due to alpha deposition
  - Improved understanding of Pt. Design's initial perturbations that can lead to the mix
  - Modified designs that show promise of improved performance
- **Complex Hohlraum Physics:** **2012**: Long pulse, gas filled hohlraum with >16% Laser Plasma Instabilities (LPI): Reduced **drive**, complicated **symmetry** control, hot electron (**preheat**)
  - **2014**: Potentially better hohlraums, with shorter pulse & less gas fill, show reduced LPI, reduced hot electrons, better understood drive, & possibly better symmetry control
    - These are natural choices for alternate ablators like High Density Carbon (HDC) or Be
      - After 2 DT shots, HDC has > 3x more yield than 2012 CH, so far, – with "head-room" for improvements

Recent progress shows the benefits of innovation, and exploration of broad approaches. This can lead to even better performance, and we've barely begun to innovate !

From National Ignition Facility & Photon Science
"Experimental Highlights: 2017 (March 2017):"

Since 2015, the ICF team has made significant strides in understanding these issues through a combination of creative experimental techniques and integrated experimental tests. Progress was made in demonstrating symmetry control in three out of four separate experimental campaigns. In addition, progress was made on reducing LPI, increasing hohlraum efficiency, and investigating alternative target supports and fill-tube configurations (see, for example, "Riding 'Unicorns' Into the Future for NIF"). These efforts will be discussed in future articles in this series.

Looking to 2017, the researchers will be building on their prior progress by evaluating different capsule materials (plastic, diamond, and beryllium), continuing to examine how to optimize each capsule to the hohlraum configuration that works best with it, and looking for and understanding performance cliffs.

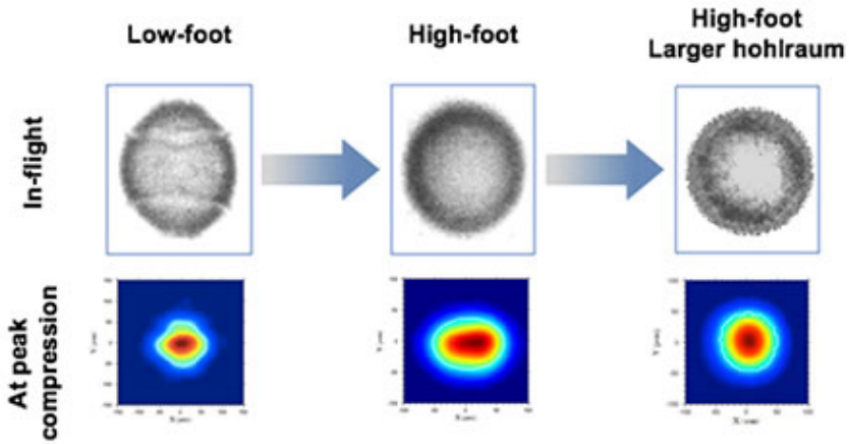

In the original "low-foot" design, the implosion was asymmetric as evidenced by the x-ray snapshot taken when the capsule was imploded to about 1/5 of its original radius (top) and the capsule support tents seeded perturbations in the shell in-flight which then fed into the hot spot later in time (x-ray emission image, bottom). The "high-foot" was less sensitive to the tent, but control of symmetry remained a challenge. More recent high-foot implosions in a larger hohlraum have shown good spherical symmetry throughout the implosion, from in-flight to peak compression. To provide better understanding of these factors, the focus also is on developing and installing improved diagnostics.

"Fast ignition" is an alternative to "hot spot ignition"

- Capsule is compressed on low adiabat
- Second "igniter" pulse starts ignition process

Compression pulse:
Pulse energy ~ 200 kJ – 1 MJ
Pulse duration ~ 10 ns
Spot radius ~ 2 mm

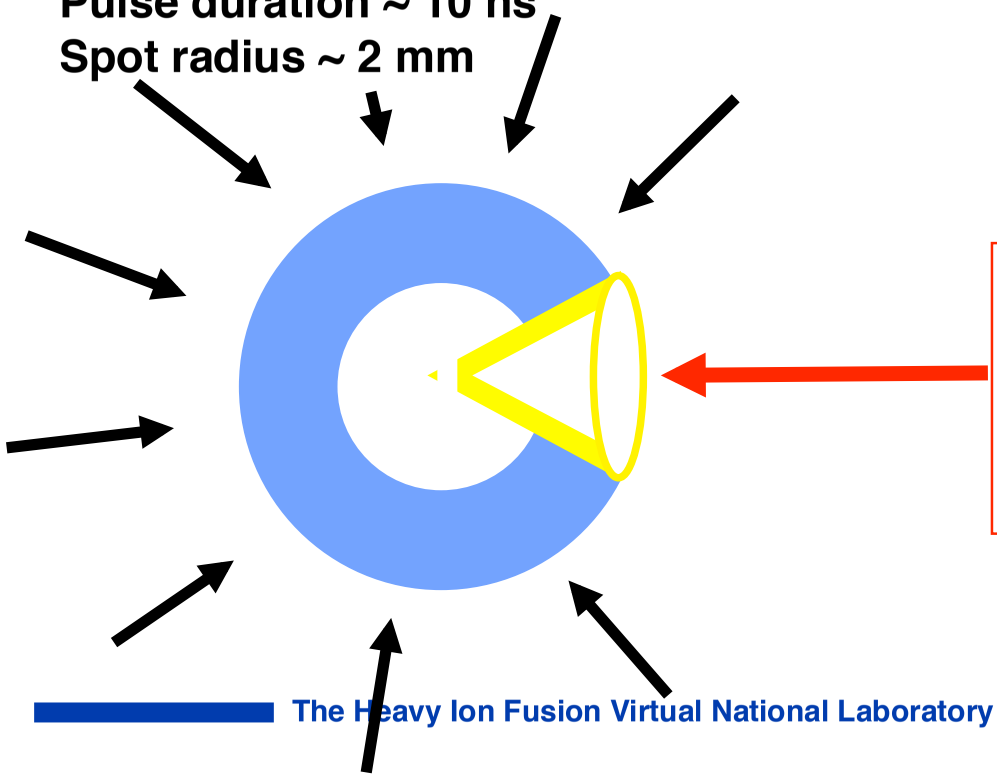

Igniter pulse: (creates electron or ion beam)
Pulse energy ~ 200 kJ – 1 MJ
Pulse duration ~ 20 ps
Spot radius ~ 20 μ

The X-Target-Mark2: XMK2

20 GeV Rubidium beams (0.5+0.5+2.0 = 3.0 MJ)
Yield = 1.2 GJ

1st, 2nd, and ignition beams are many beams with overlapping spots modeled as annuli

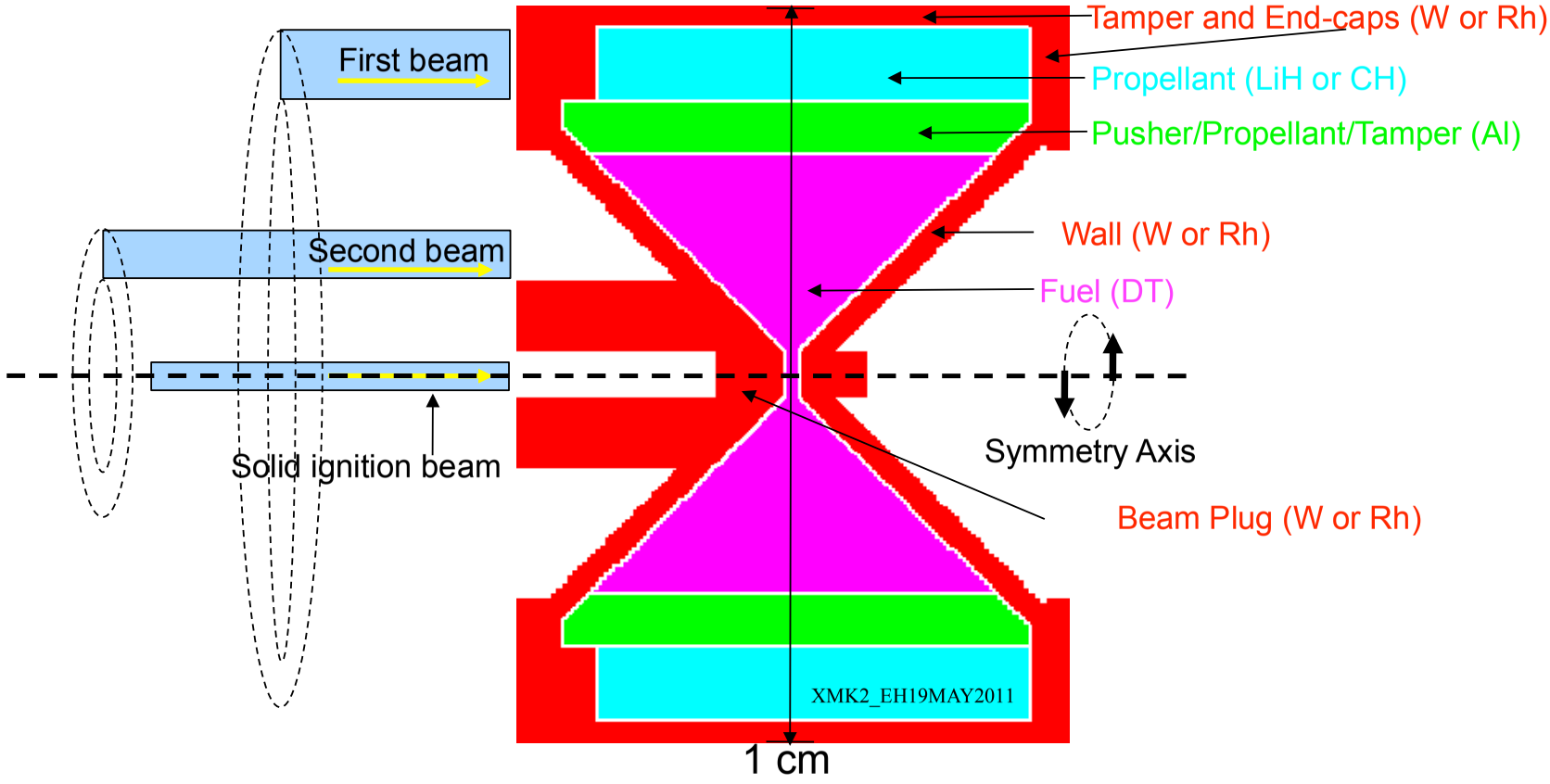

A "distributed radiator" target produces high gain in radiation/hydrodynamic simulations

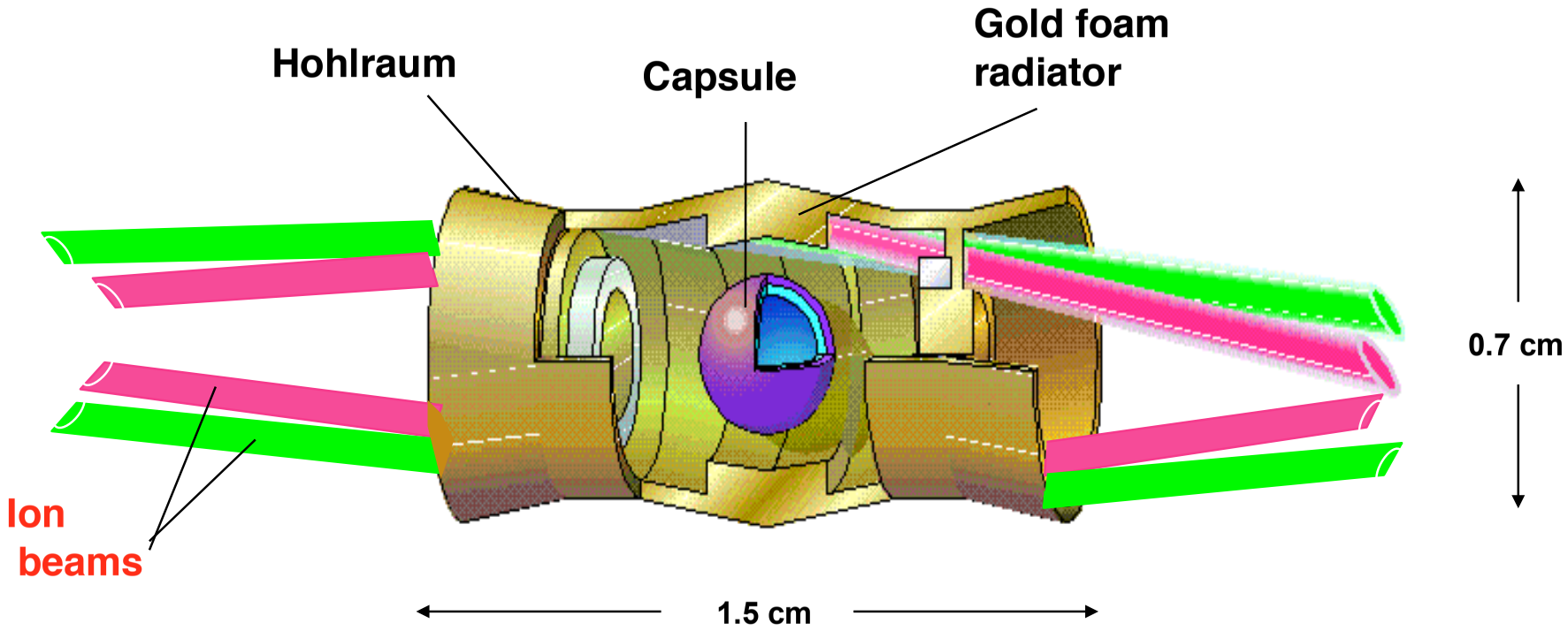

Overlapping Gaussian, elliptical beams are focused at the end of the target

Each beam is an ellipse

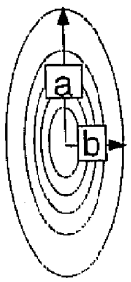

8 beams overlap in the foot pulse

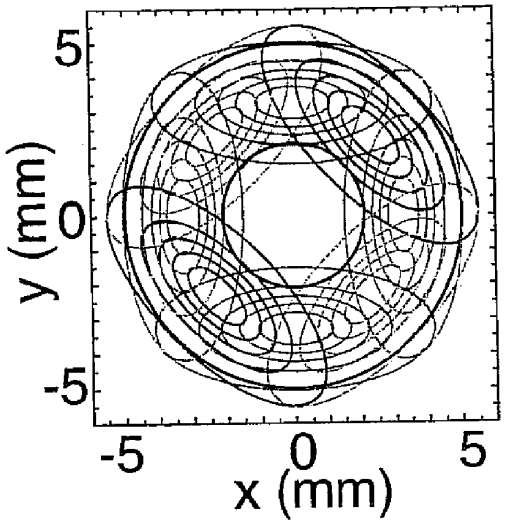

Sum of 8 foot pulse beams

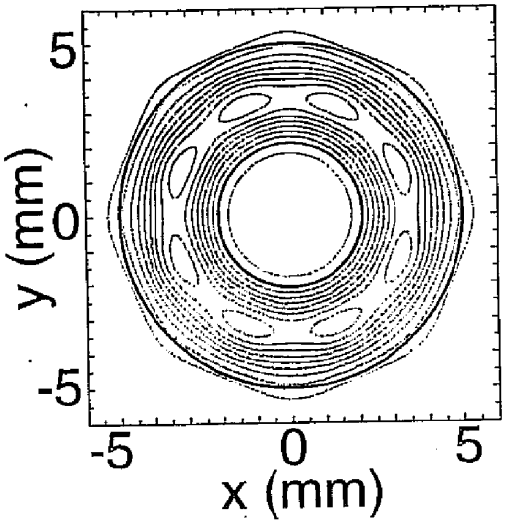

a = 4.15 mm
b = 1.8 mm
effective r=2.7 mm
95% of charge inside

Azimuthal asymmetry:
foot pulse: -1.6% in m=8
main pulse: 0.06% in m=16

Ion current profile and radiation temperature

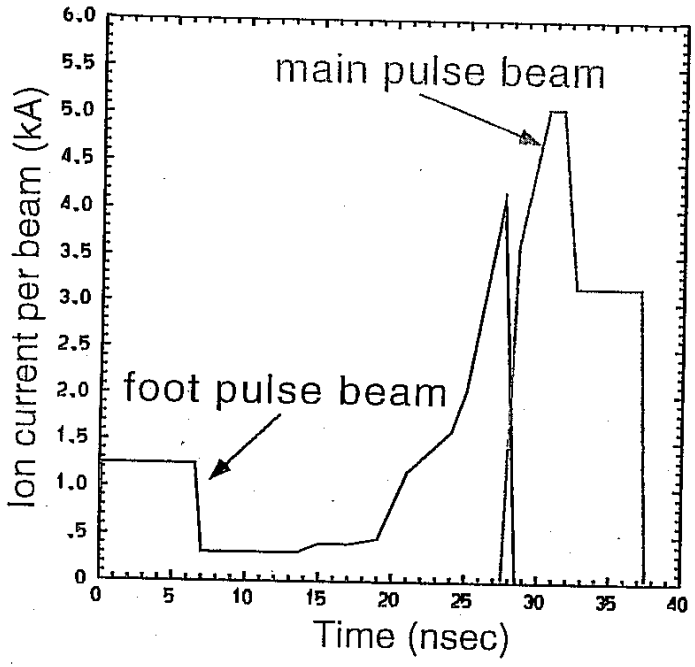

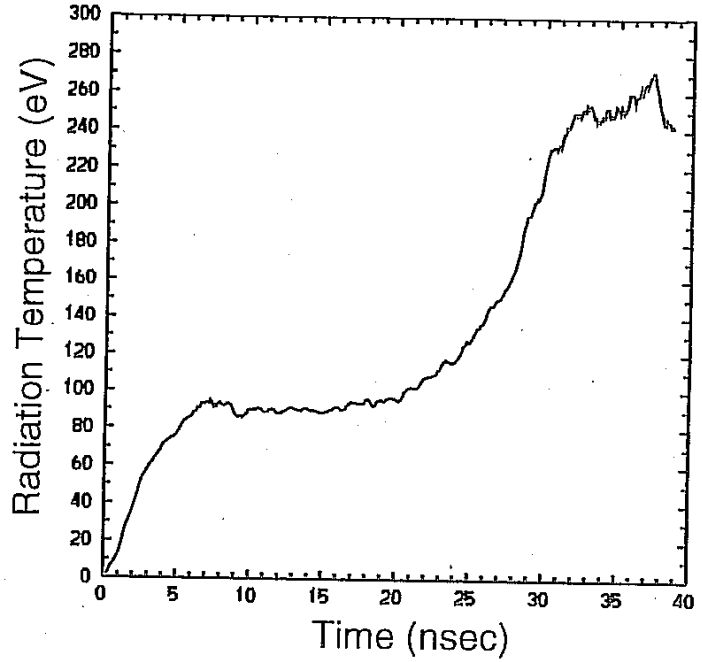

Current assumes 16 beams in foot pulse
32 beams in main pulse

Why heavy ions?

Target requires:

3 – 6 MJ in ~ 10 ns => Power ~500 TW
Range ~ 0.02 – 0.2 g/cm^2

Range relation:
Higher ion mass => higher ion energy (for fixed range)

Power relation:
Power = ion energy x ion current => Higher ion energy requires lower current (for fixed power)

Minimize current to ease transport and focusing of beams

Heavier Ions ⇒ Higher Kinetic Energy

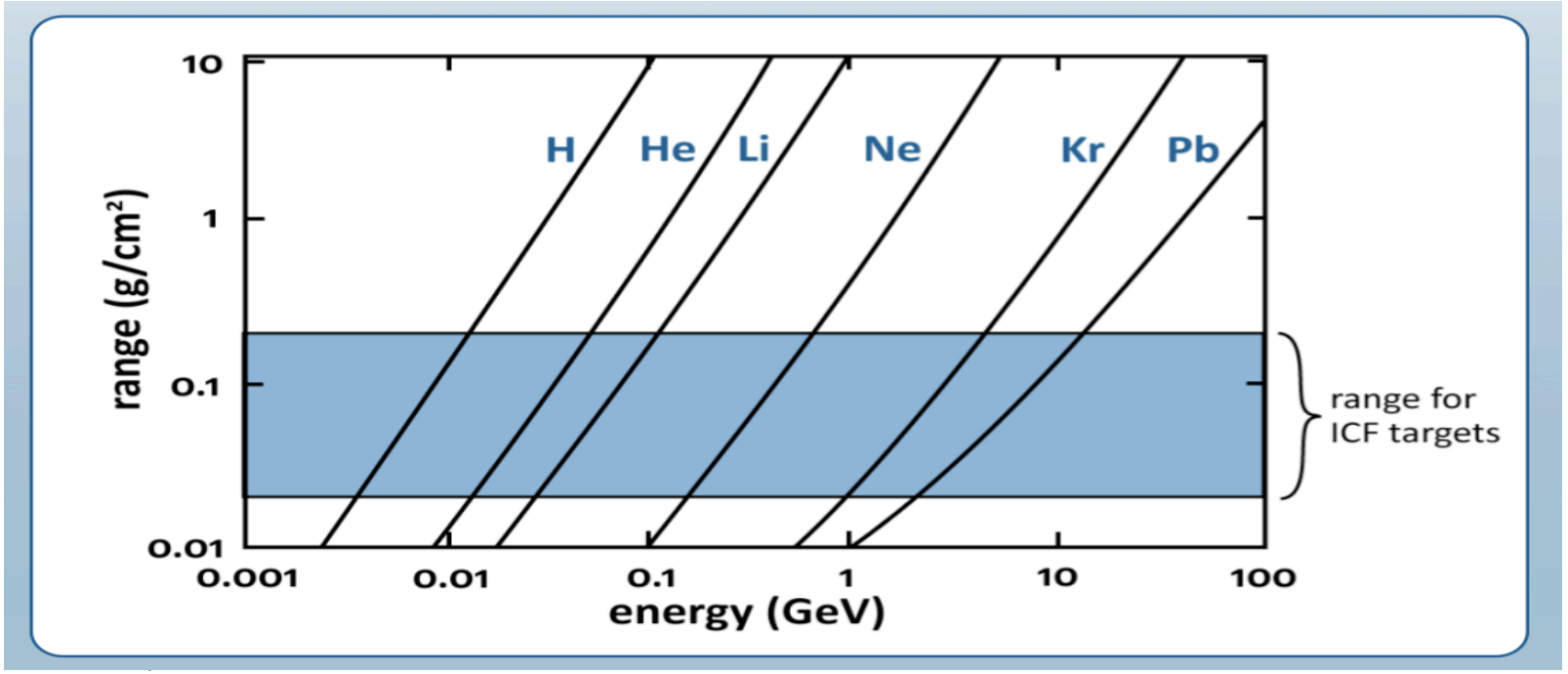

Targets require high power (kinetic energy x current).

- **Light Ion Fusion requires high-current, unconventional accelerators (Sandia 1970s).**
- **Heavy Ion Fusion requires lower currents enabling the use of more conventional high energy accelerators (Maschke ~ 1974).**

There are two principle methods of acceleration

1. r.f. acceleration

(Approach in Europe and Japan)

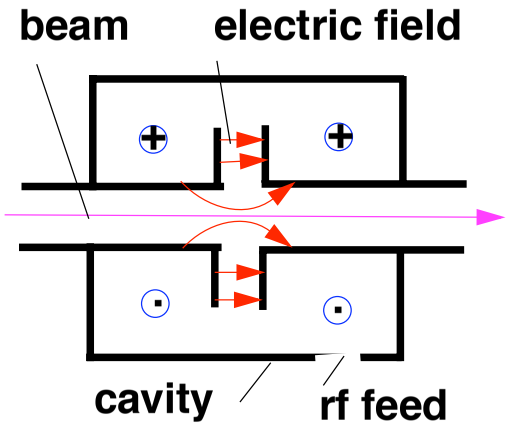

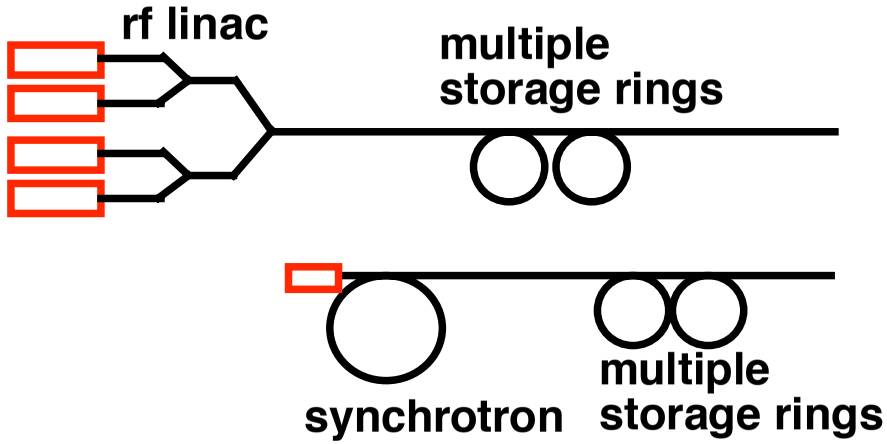

2. Induction acceleration

(U.S. approach)

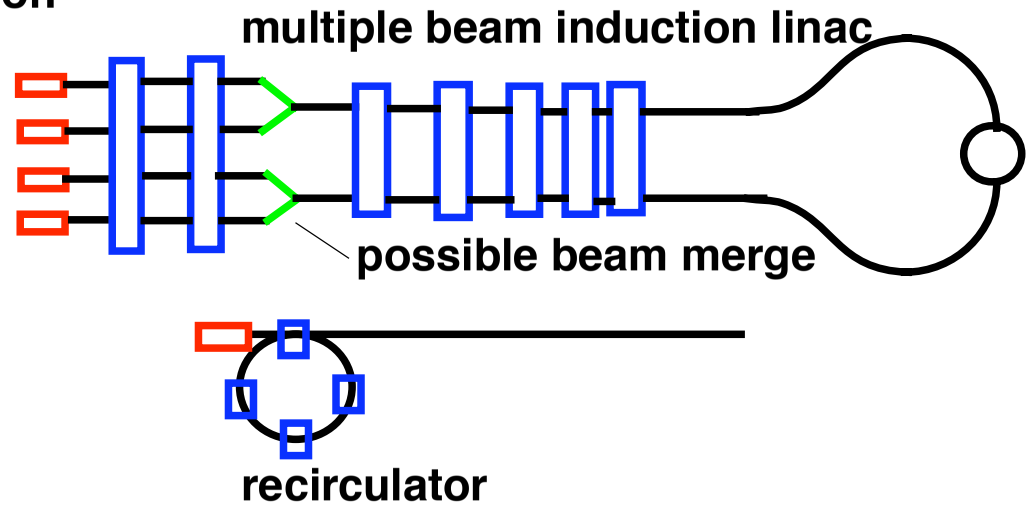

Induction acceleration for HIF consists of several subsystems and a variety of beam manipulations

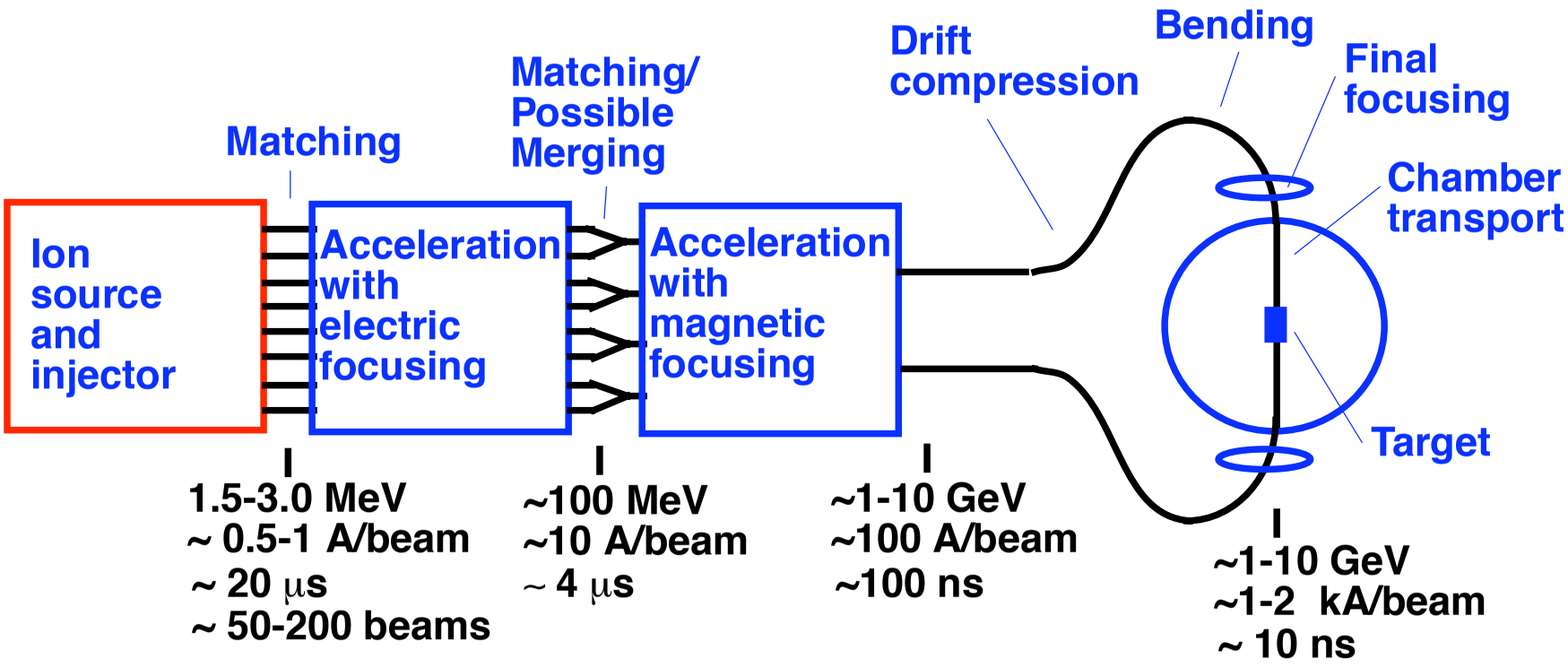

A "Robust Point Design" design study established a baseline for a multibeam quadrupolar linac HIF driver

Typical Driver Parameters:

1.6 MeV, Bi (mass 209)
0.6 A/beam
30 μs
120 beams

4 GeV
200 A/beam
200 ns

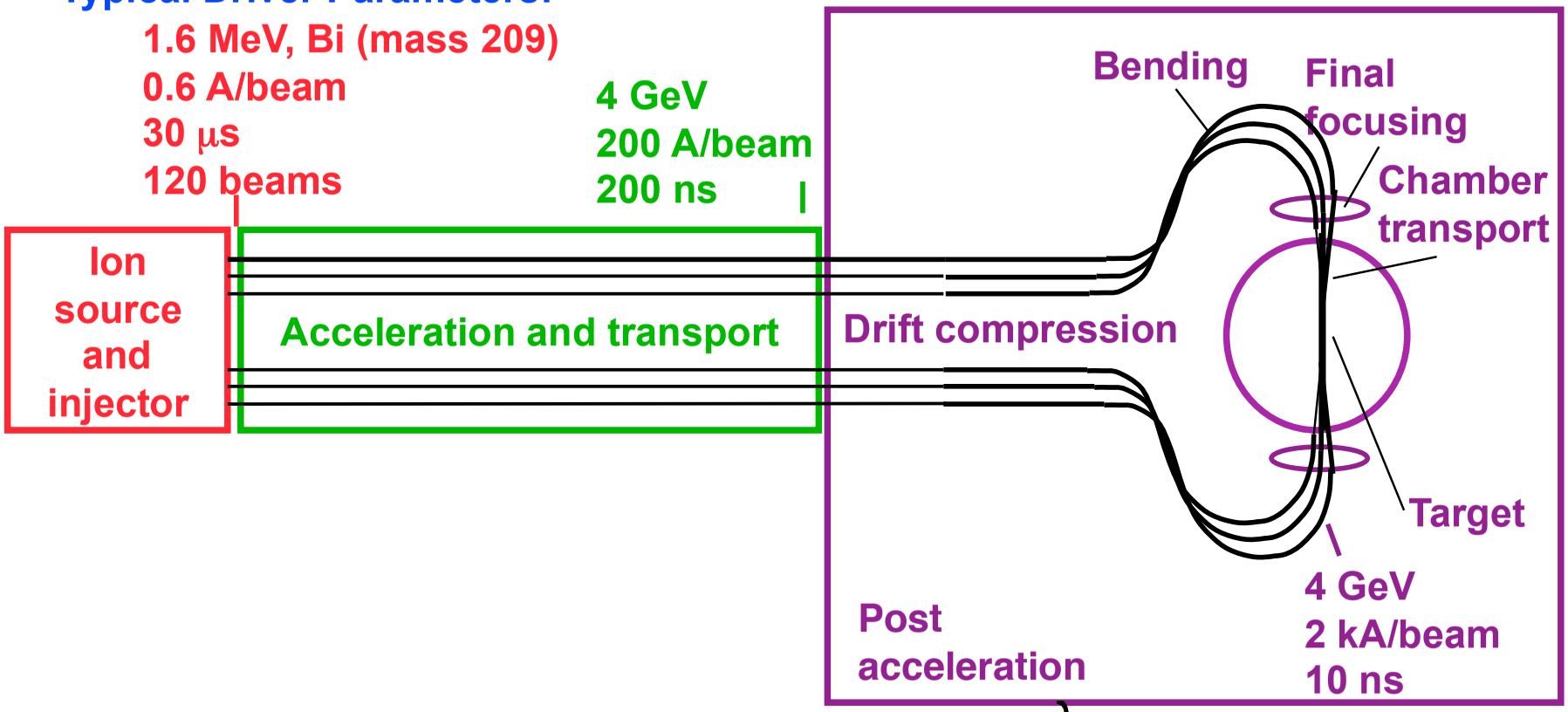

Relative bunch length at end of:

injector

accelerator

drift compression

Summary of Current Limits From Different Focusing Methods

Einzel Lens

$$Q_{max} \cong \frac{3\pi^2}{\gamma}\left(\frac{qQ_0}{mV_0^2}\right)^2\left(\frac{r_b}{L}\right)^2$$

Solenoids

$$Q_{max} = \left(\frac{\omega_c r_b}{2V\beta c}\right)^2$$

Quadrupole Focusing

$$Q_{max} \cong \frac{\eta\sigma_0}{2\pi}\left(\frac{\sin\frac{\eta\pi}{2}}{\frac{\eta\pi}{2}}\right)\left[\frac{Br_b}{[B\rho]}\left[\frac{r_b}{r_p}\right]\right.$$ (Magnetic)

$$\left.\frac{2qV_q}{\gamma mV_z^2}\left[\frac{r_b^2}{r_p^2}\right]\right]$$ (Electric)

For Non-Relativistic Beams

$$\lambda_{max} \propto \frac{Q_0^2}{V}$$

$$\lambda_{max} \propto \frac{q}{m}B^2 r_p^2$$

$$\lambda_{max} \propto \begin{cases} B, V^{1/2} r_p \\ V_q \end{cases}$$

Note
- Q_0 = Voltage between Einzel lenses
- V_q = Voltage on a quad relative to ground
- V = particle energy / q

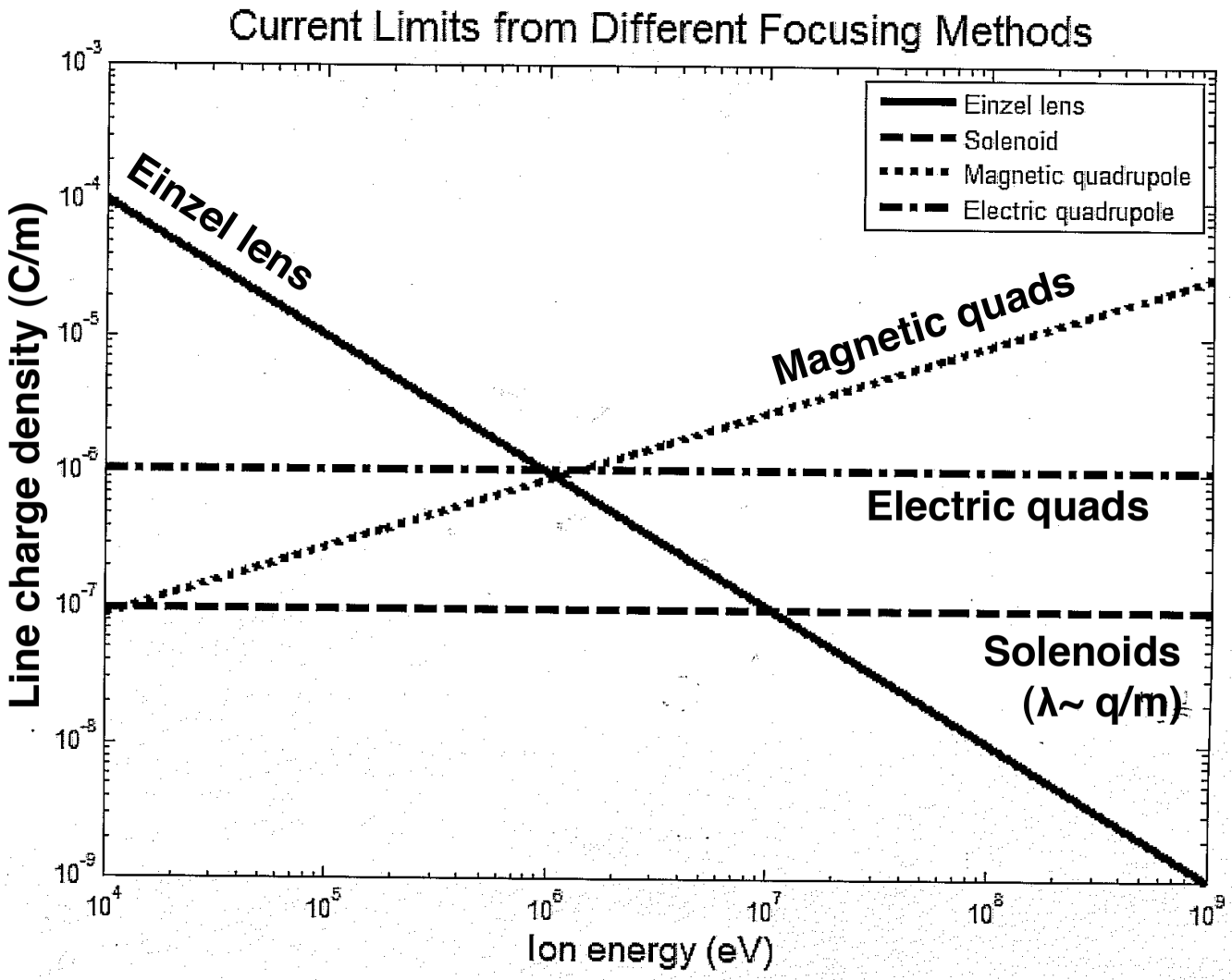
Current Limits from Different Focusing Methods
Einzel lens
Solenoid
Magnetic quadrupole
Electric quadrupole
Einzel lens
Magnetic quads
Electric quads
Solenoids
(λ~ q/m)
Line charge density (C/m)
Ion energy (eV)
10^-3
10^-4
10^-5
10^-6
10^-7
10^-8
10^-9
10^4
10^5
10^6
10^7
10^8
10^9

Major components of induction linac

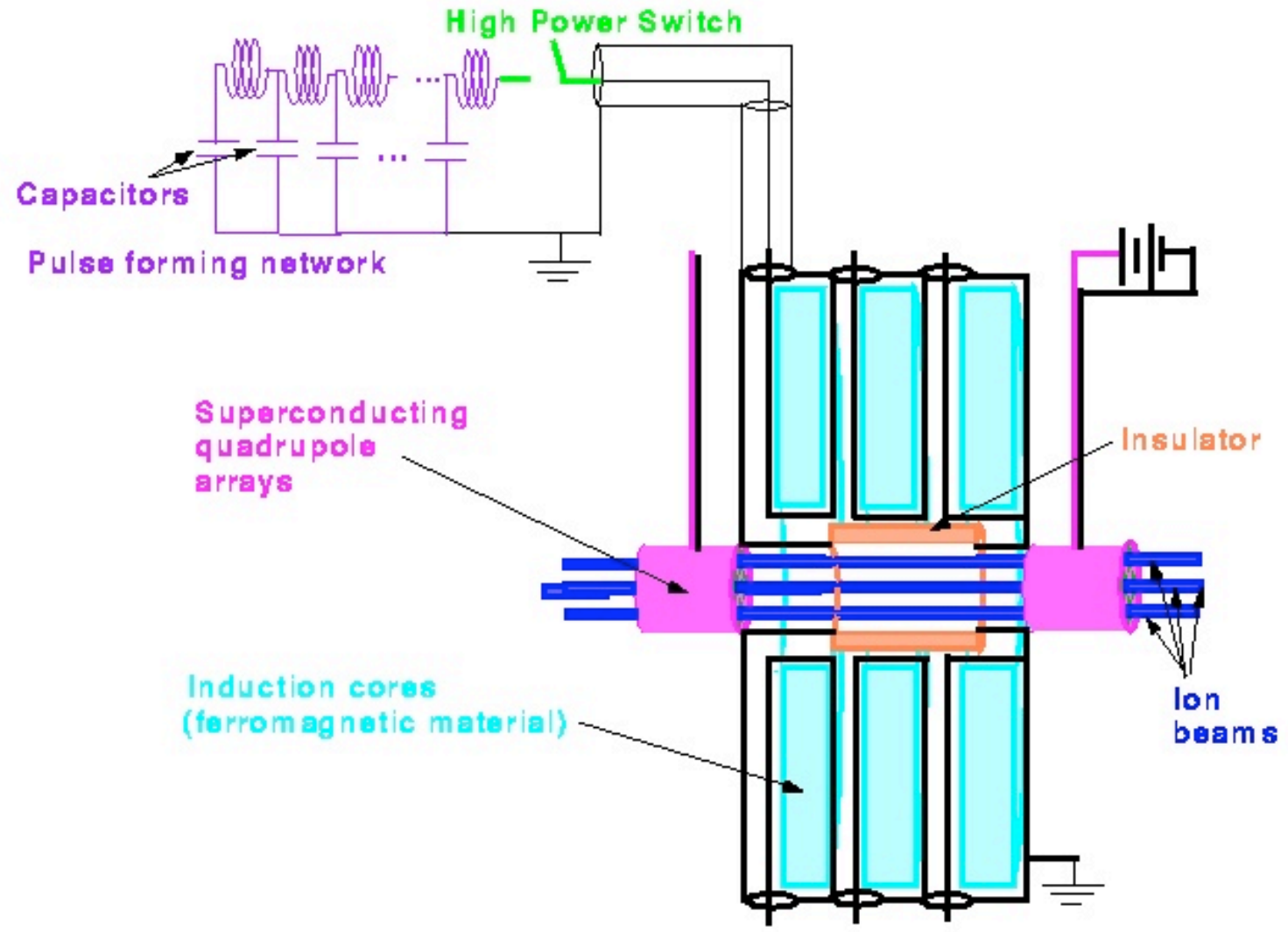

An Induction Core

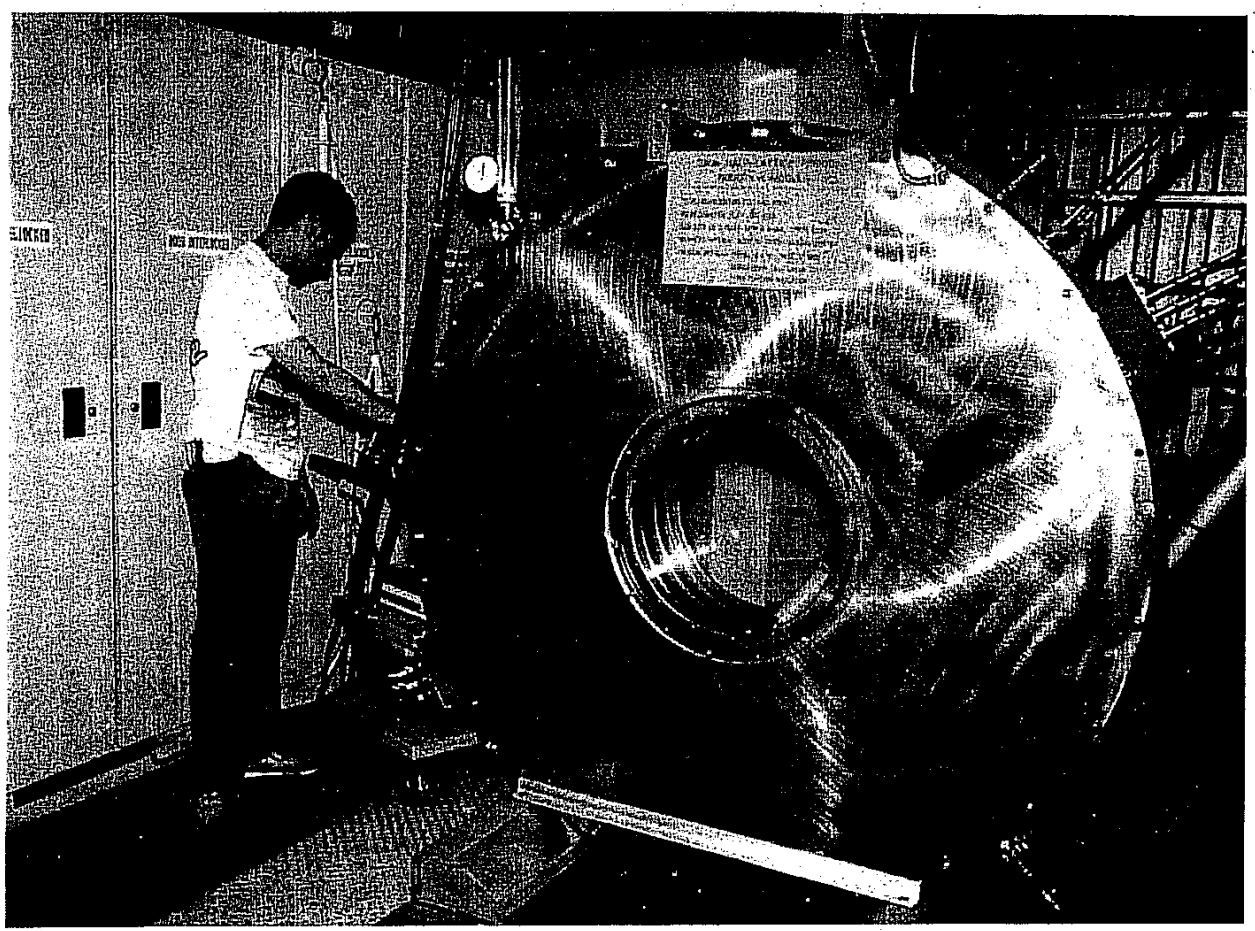

An array of small beamlets maximizes the current that can be transported through an induction core

From class, for magnetic quadrupoles:

$$Q_{\max} \cong \frac{\eta\sigma_0}{2\pi}\left(\frac{\sin\frac{\eta\pi}{2}}{\frac{\eta\pi}{2}}\right)\frac{B}{[B\rho]}\left(\frac{r_b}{r_p}\right)r_b$$

$$\Rightarrow \lambda_{\max} \propto \left(\frac{qV}{m}\right)^{1/2} B\left(\frac{r_b}{r_p}\right)r_b$$

$$\Rightarrow I_{\max} = \beta c\lambda_{\max} \propto \left(\frac{qV}{m}\right)B\left(\frac{r_b}{r_p}\right)r_b$$

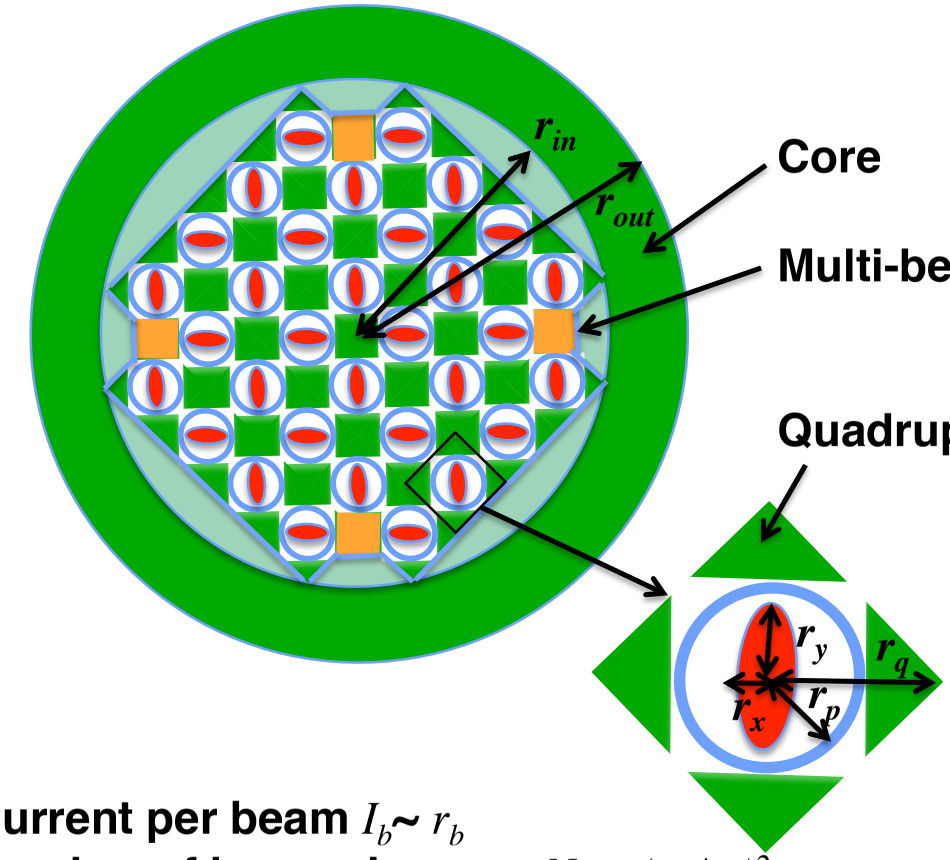

Beam pipe radius = r_p
Beam radius = r_b

Current per beam $I_b \sim r_b$
Number of beams in array $N_b \sim (r_{in}/r_b)^2$
Total current through core = $I_{tot} \sim N_b I_b \sim r_{in}^2/r_b$ **until** r_p/r_b **= constant no longer applies)**
(Better scaling $r_p \sim C_1 r_b + C_2$ **but basic idea still applies until)**

A Typical driver has about 2000 individual modules

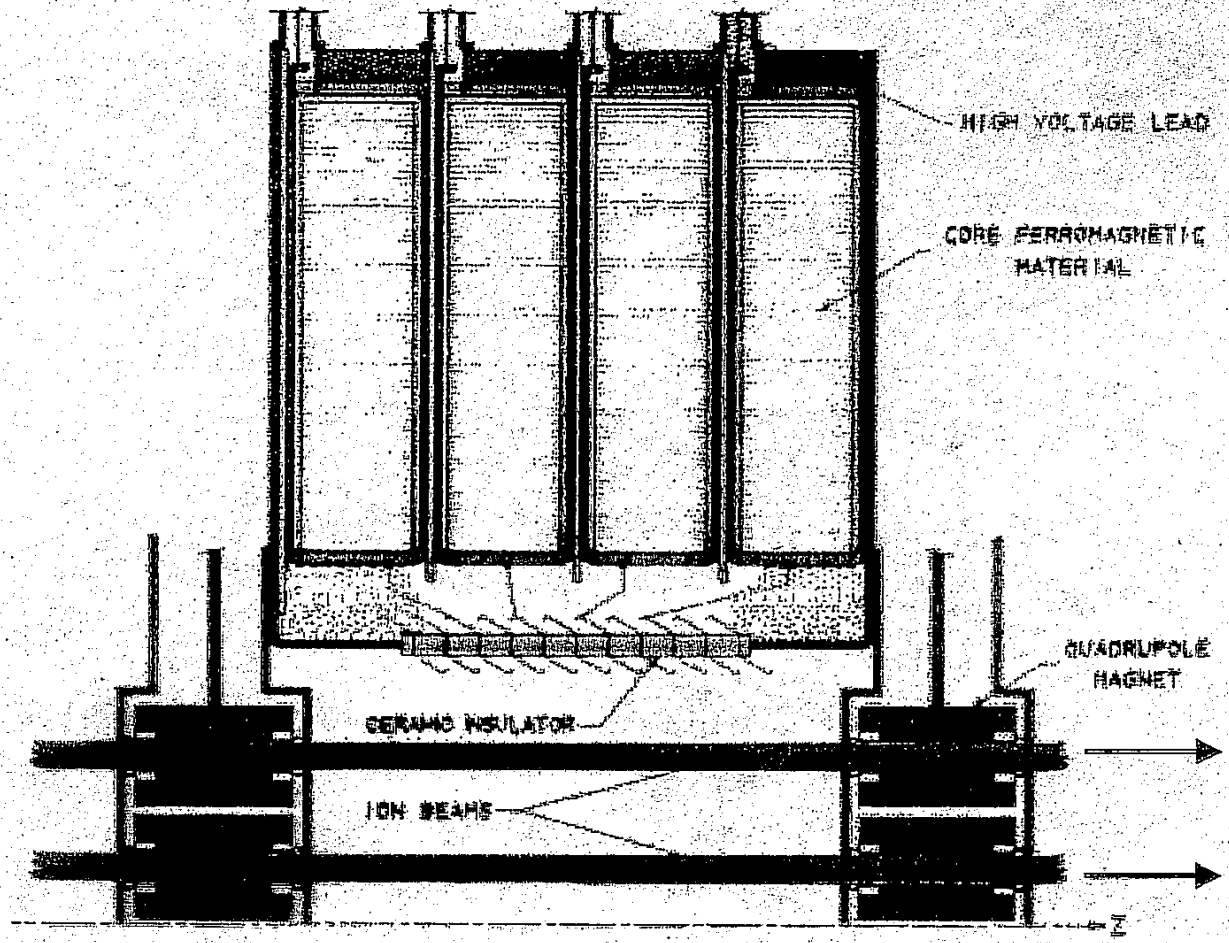

In induction linac, there are several limits that constrain design

Phase advance per lattice period $\sigma_0 < 85^o$ **(to avoid envelope/lattice /higher order mode instabilities and emittance growth)**

Space charge is limited by external focusing $Q < (\sigma_0 r_b/(2L))^2$ **where** Q **is the perveance,** r_b **is average beam radius, and** L **is the half-lattice period**

Velocity tilt cannot be too large (to avoid beam head-to-tail mismatches) ($\Delta v/v_0 <\sim 0.3$ **for electric quadrupoles)**

"Volt-seconds/meter" $(dV/ds\ l/v_0 <\sim 1.5\text{ -}2.0\ V\text{-}s/m)$ **(for reasonable induction core sizes).**

Voltage gradient dV/ds **<~ 1 MV/m (also for reasonable core sizes and avoiding breakdown limits)**

Sources of non-linearity and mismatch are well defined

Sources of non-linearities

- External focusing magnets
- Space-charge
- Multiple-beam effects

Sources of mismatch

- Accelerator imperfections
  - Quad strength and placement errors
  - Acceleration waveform errors
  - Bend strength errors
- Velocity tilt

Simulations give reliable and definitive tolerances on each source

Several potential instabilities have been investigated in HIF drivers

Temperature anisotropy instability

After acceleration $T_{||} << T_{\perp}$, internal beam modes are unstable; saturation occurs when $T_{||} \sim T_{\perp}/3$

Longitudinal resistive instability

Module impedance interacts with beam, amplifying space-charge waves that are backward propagating in beam frame

Beam break-up (BBU) instability

High frequency waves in induction module cavities interact transversely with beam

Beam-plasma instability

Beam interacts with residual gas in target chamber

All of these instabilities have known analytic linear growth rates, which constrain the accelerator design (to ensure minimal growth or benign saturation).

One option for final drift compression is to use a current pulse that is flat with parabolic ends (modeled using the HERMES code)

15 ns final pulse duration

The initial tilt on the beam is about 4% (compare to ~30% at the beginning of the accelerator)

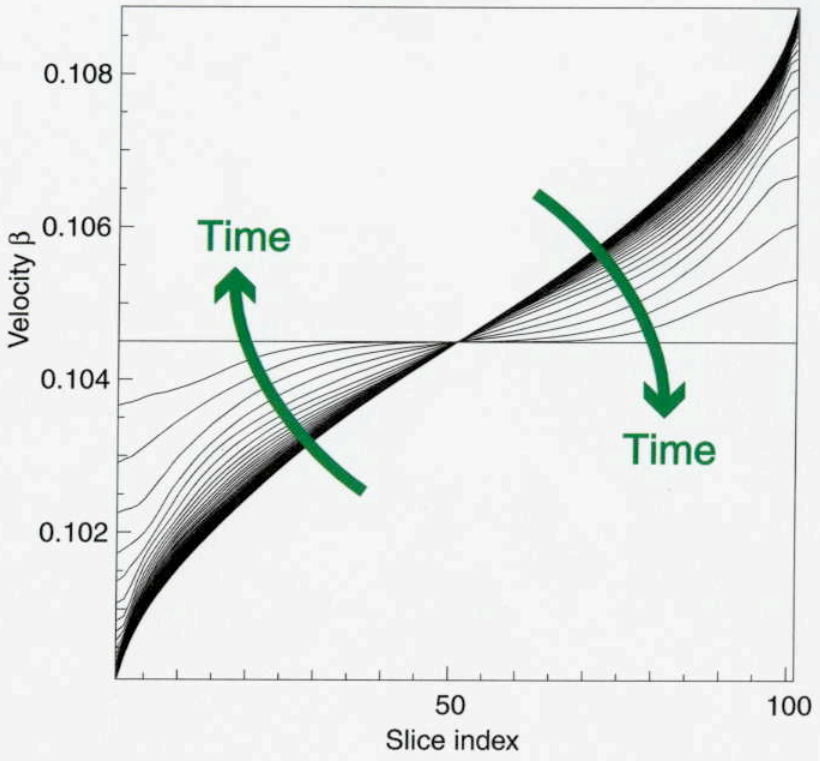

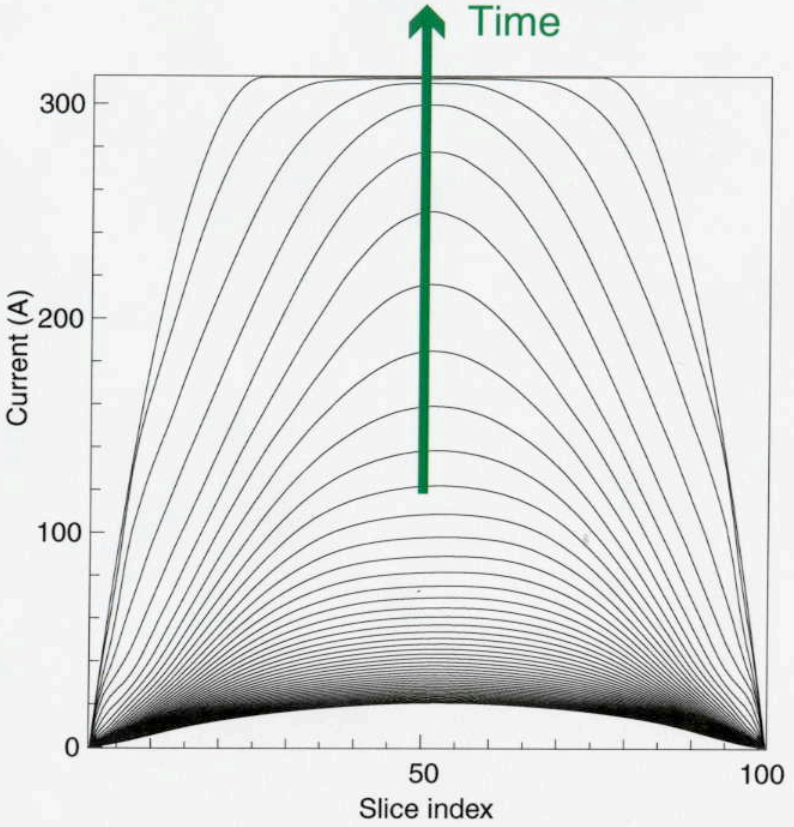

Although the final beam profile is flat, it is parabolic for most of the drift compression

Drift compression section is designed by running code first backwards from target, then forwards after rematching

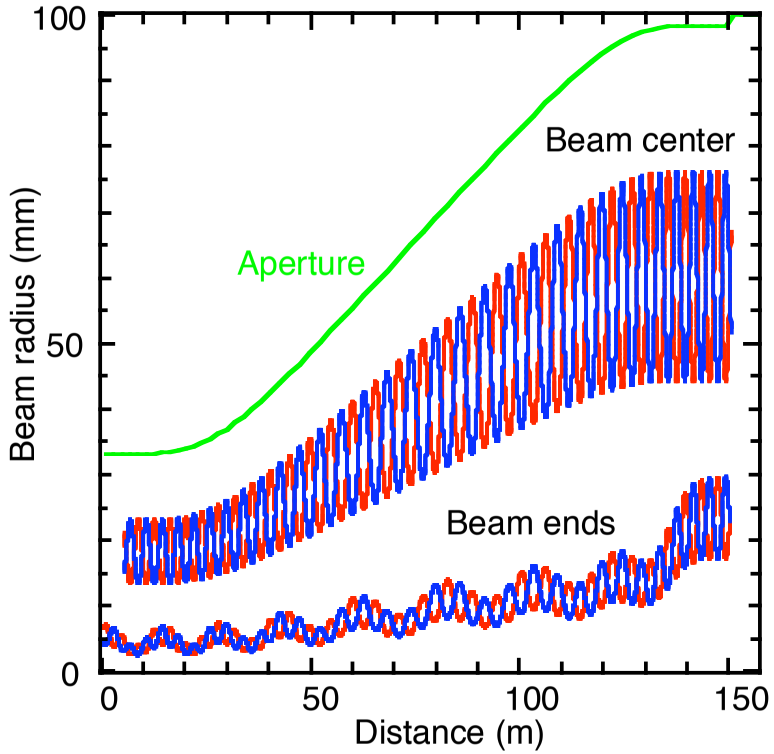

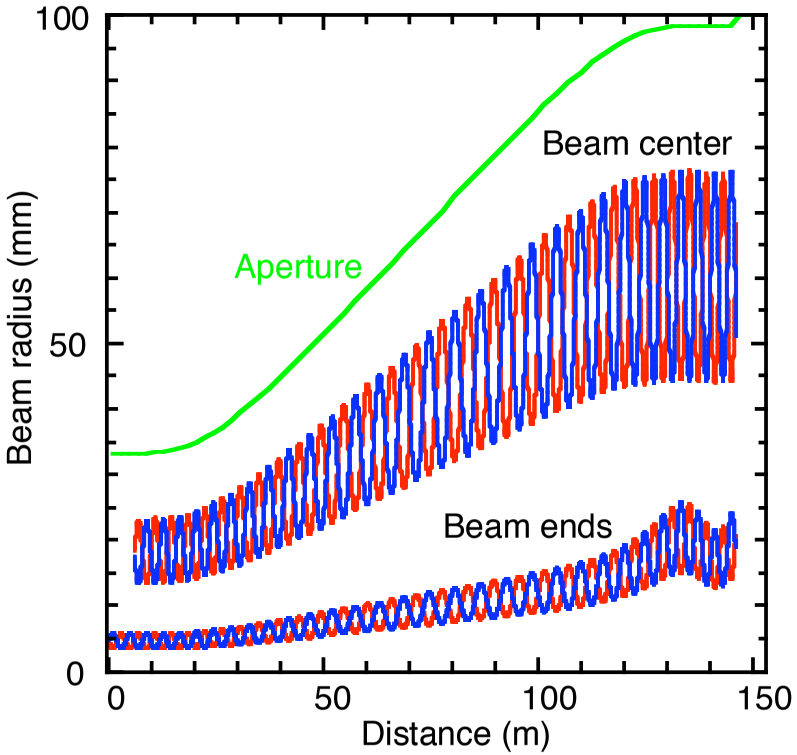

Begin with a desired 20ns, constant -energy pulse at end of compression, track backwards, design lattice for central slice; beam end becomes mismatched early on

"Rematch" at entrance to compression section, by adjusting a,a',b,b'; then track forward

Heavy ion fusion chamber designs envision using neutronically thick liquid walls to protect solid wall

HYLIFE II chamber concept:

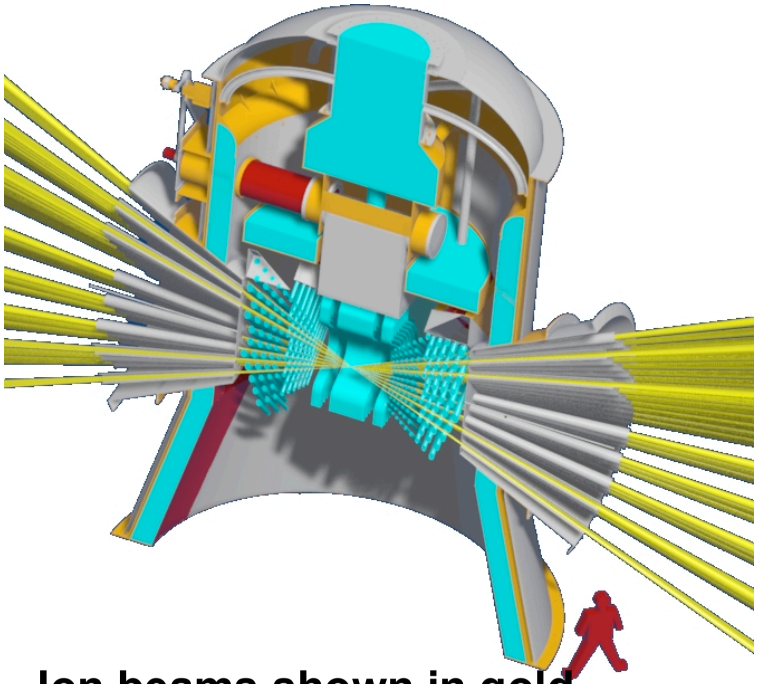

Jets provide protection in vicinity of beamlines

Pocket forms from oscillation of nozzles

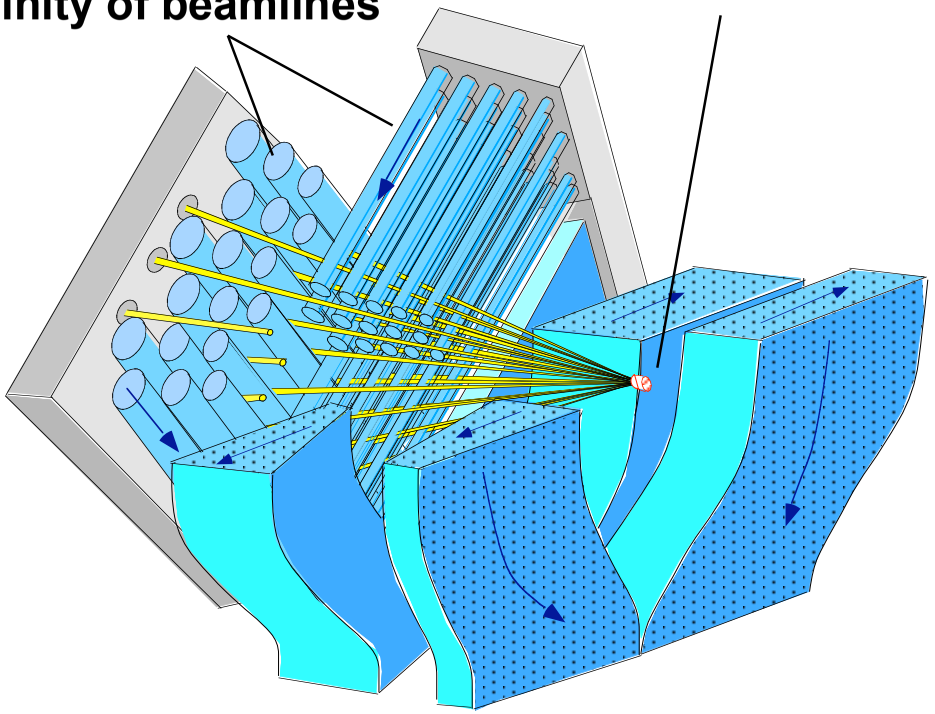

Ion beams shown in gold
FLiBe (a liquid salt) shown in turquoise

Several options exist for quadrupole based final focus for HIF application

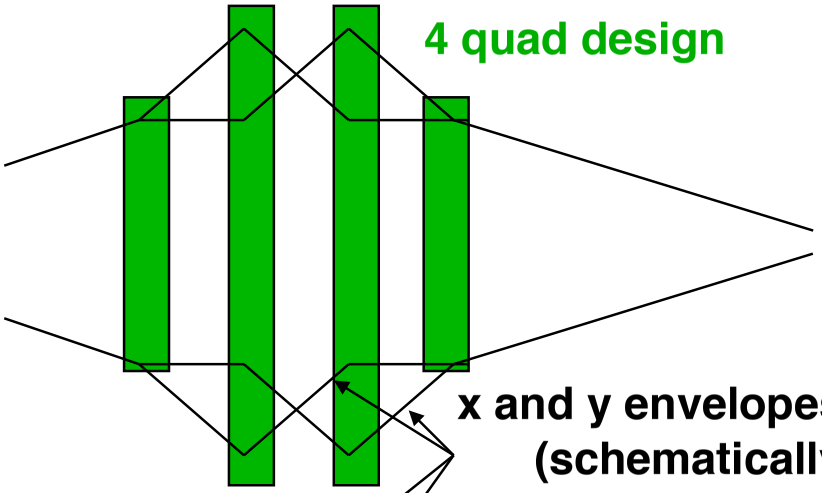

4 quad design

x and y envelopes (schematically depicted)

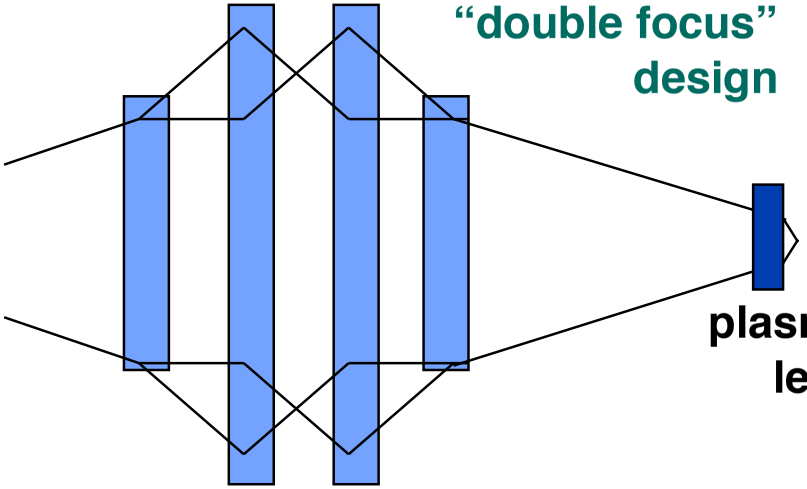

"double focus" design

plasma lens

could increase spot heating for target heating studies

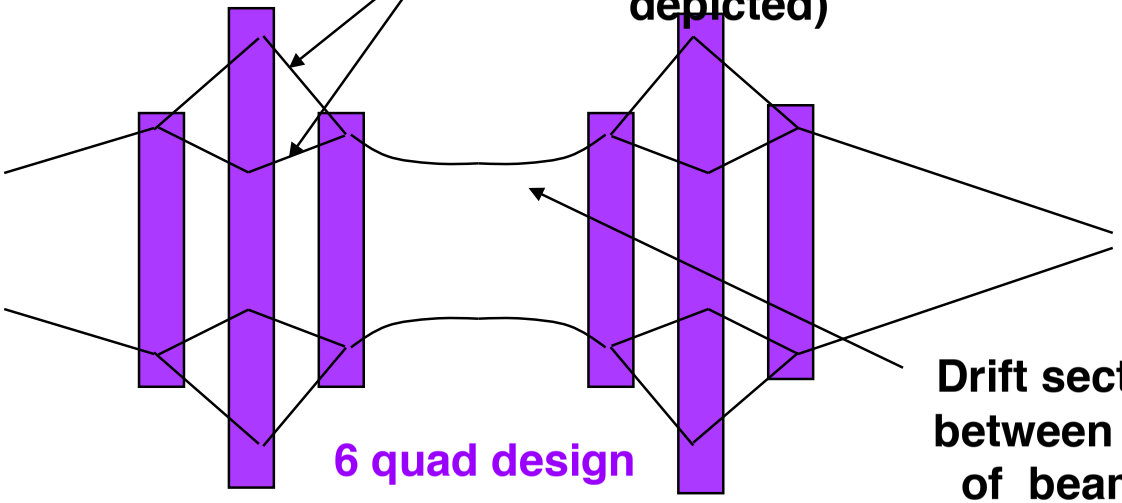

6 quad design

Drift section with circular beam between triplets allows rotation of beams or insertion of bend

ESTIMATING SPOT SIZE

$$r_x'' + \frac{(\gamma_b \beta_b)'}{\gamma_b \beta_b} r_x' + k_x r_x - \frac{2Q}{r_x + r_y} - \frac{\varepsilon_x^2}{r_x^3} = 0$$

$$r_y'' + \frac{(\gamma_b \beta_b)'}{\gamma_b \beta_b} r_y' + k_y r_y - \frac{2Q}{r_x + r_y} - \frac{\varepsilon_y^2}{r_y^3} = 0$$

IN CHAMBER: NO EXTERNAL FOCUSING, NO ACCELERATION AND BEAM IS OFTEN CIRCULAR (BY DESIGN)

$\Rightarrow k_x = k_y = (\gamma_b \beta_b)' = 0$ & $r_x = r_y = r_b$

$\Rightarrow$ ENVELOPE EQUATION IS:

$$r_b'' = \frac{Q}{r_b} + \frac{\varepsilon^2}{r_b^3}$$

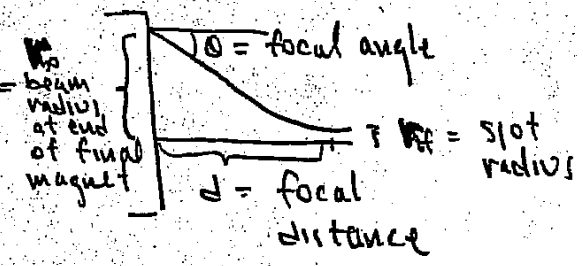

MULTIPLYING BY r_b' & INTEGRATING $\Rightarrow$

$$\frac{r_{bf}'^2}{2} - \frac{r_{b0}'^2}{2} = Q \ln \frac{r_{bf}}{r_{b0}} + \frac{\varepsilon^2}{2 r_{b0}^2} - \frac{\varepsilon^2}{2 r_{bf}^2}$$

NOW $r_{b\theta}' \cong \theta$ $\quad r_{bf}$ = spot radius $\quad r_{bf} \ll r_{b0}$

$r_{bf}' = 0$ $\quad r_{b0} \cong d\theta$

$$\Rightarrow \boxed{\theta^2 \cong 2Q \ln\left(\frac{\theta d}{r_{bf}}\right) + \frac{\varepsilon^2}{r_{bf}^2}}$$

FOR EMITTANCE DOMINATED SPOT: $r_{bf} = \frac{\varepsilon}{\theta}$

"CHROMATIC ABERRATIONS" TEND TO BROADEN SPOT

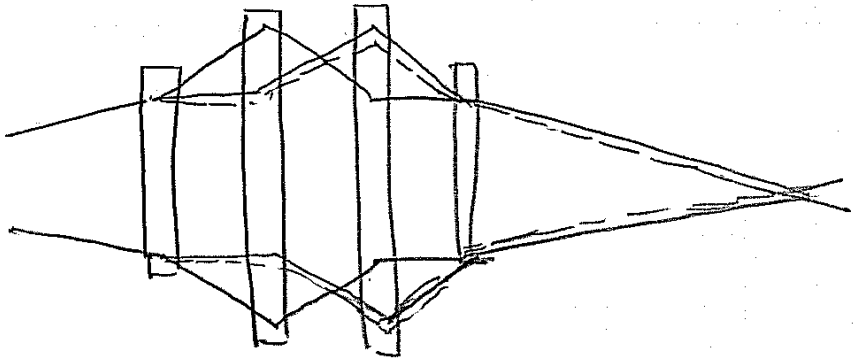

SINCE QUADRUPOLE MAGNET FOCUSING $\propto \frac{1}{V_z}$

(i.e. $x'' = \frac{qB'}{\gamma m V_z} x$) A SPREAD IN LONGITUDINAL VELOCITY GIVES RISE TO A BROADENING OF FINAL SPOT.

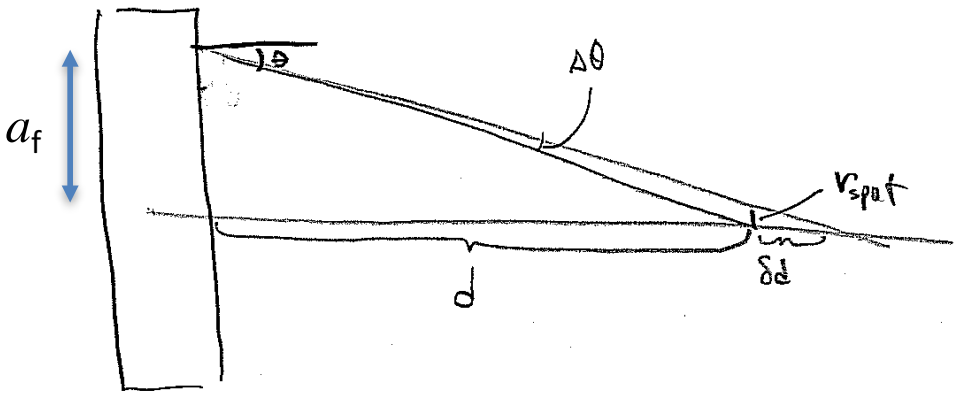

e.g. $\theta d = a_f$

$$\Rightarrow \frac{dd}{d\theta} = \frac{-a_f}{\theta^2} = \frac{-d}{\theta}$$

and $\Delta x' = \theta = \frac{const}{p}$

$$\Rightarrow \frac{d\theta}{dp} = -\frac{const}{p^2} = -\frac{\theta}{p}$$

$$r_{spot} = \theta\, \delta d$$
$$= \theta \frac{\partial d}{\partial \theta} \frac{\partial \theta}{\partial p} \delta p$$
$$= \alpha\, \theta d \left(\frac{\delta p}{p}\right)$$

α = some constant depending on focal system

HEURISTICALLY THE CONTRIBUTION FROM CHROMATIC ABERRATIONS CAN BE WRITTEN

$$\sigma_{chrom}^2 = \alpha^2 D^2 \left(\frac{\delta\gamma}{\gamma}\right)^2 \theta^2$$

where α depends on system, typically 4-8

$$\sigma_{spot}^2 = \sigma_{bf}^2 + \sigma_{chrom}^2$$

DETAILED SIMULATIONS OR MOMENT CODE RESULTS REQUIRED TO FIX α.

How can we estimate the coefficient for chromatic aberrations?

We constructed moment models to study chromatic effects (through 2nd order) in final focus system

$$\frac{dp_x}{dt} = q(E_x + v_z B_y - v_y B_z)$$

Expand through 2nd order in x', y', $k_{\beta 0}x$, $k_{\beta 0}y$, $\delta p/p$

$$x'' + \left(\frac{1}{\gamma v_{z0}}\frac{d}{dz}(\gamma v_z)\right)x' \cong \frac{qB'}{\gamma m v_{z0}}x\left(1-\frac{\delta p}{p}\right) + \frac{q\lambda}{4\pi\varepsilon_0 m v_{z0}^2}\frac{(x-\bar{x})(1-\frac{2\delta p}{p})}{(\Delta x^2 + [\Delta x^2 \Delta y^2]^{1/2})}$$

The equation of motions can be written (where $\delta = \delta p/p$**) :**

$$x'' \cong K_{xx}x + K_{xx1}x\delta \qquad y'' \cong K_{yy}y + K_{yy1}y\delta$$

Here:

$$K_{xx} = \frac{B'}{[B\rho]_0} + \frac{Q}{2(\Delta x^2 + [\Delta x^2 \Delta y^2]^{1/2})} \qquad K_{yy} = \frac{-B'}{[B\rho]_0} + \frac{Q}{2(\Delta y^2 + [\Delta x^2 \Delta y^2]^{1/2})}$$

$$K_{xx1} = -\left[\frac{B'}{[B\rho]_0} + \frac{2Q}{2(\Delta x^2 + [\Delta x^2 \Delta y^2]^{1/2})}\right] \qquad K_{yy1} = -\left[\frac{-B'}{[B\rho]_0} + \frac{2Q}{2(\Delta y^2 + [\Delta x^2 \Delta y^2]^{1/2})}\right]$$

B' = **quadrupole gradient;** $[B\rho]$ = **Ion rigidity** $= p/q$; Q = **perveance** $= \frac{q\lambda}{2\pi\varepsilon_0 \gamma_0^3 m v_{z0}^2}$

We take averages of 2nd, 3rd,… order quantities, forming infinite set of 1st order ode's

$$\frac{d}{ds}\langle x^2\rangle = 2\langle xx'\rangle$$

$$\frac{d}{ds}\langle xx'\rangle = \langle x'^2\rangle + \langle xx''\rangle$$

$$= \langle x'^2\rangle + K_{xx}\langle x^2\rangle + K_{xx1}\langle x^2\delta\rangle$$

$$\frac{d}{ds}\langle x'^2\rangle = 2\langle x'x''\rangle$$

$$= 2K_{xx}\langle xx'\rangle + 2K_{xx1}\langle xx'\delta\rangle$$

$$\frac{d}{ds}\langle x^2\delta\rangle = 2\langle xx'\delta\rangle$$

$$\frac{d}{ds}\langle xx'\delta\rangle = \langle x'^2\delta\rangle + \langle xx''\delta\rangle$$

$$= \langle x'^2\delta\rangle + K_{xx}\langle x^2\delta\rangle + K_{xx1}\langle x^2\delta^2\rangle$$

$$\frac{d}{ds}\langle x'^2\delta\rangle = 2\langle x'x''\delta\rangle$$

$$= 2K_{xx}\langle xx'\delta\rangle + 2K_{xx1}\langle xx'\delta^2\rangle$$

...

$$\frac{d}{ds}\langle x^2\delta^n\rangle = 2\langle xx'\delta^n\rangle$$

$$\frac{d}{ds}\langle xx'\delta^n\rangle = \langle x'^2\delta^n\rangle + \langle xx''\delta^n\rangle$$

$$= \langle x'^2\delta^n\rangle + K_{xx}\langle x^2\delta^n\rangle + K_{xx1}\langle x^2\delta^{n+1}\rangle$$

$$\frac{d}{ds}\langle x'^2\delta^n\rangle = 2\langle x'x''\delta^n\rangle$$

$$= 2K_{xx}\langle xx'\delta^n\rangle + 2K_{xx1}\langle xx'\delta^{n+1}\rangle$$

=> term higher order by one

Infinite set of equations can be truncated, but are reliable over only finite distances

Two equivalent methods of truncation have been employed:

1. $\langle x^2\delta^2\rangle \approx \langle x^2\rangle\langle\delta^2\rangle$ **and** $\langle xx'\delta^2\rangle \approx \langle xx'\rangle\langle\delta^2\rangle$ **; or**
2. **Noticing that** $\frac{1}{1+\delta} = 1-\delta+\delta^2+\ldots$ **and** $\frac{1}{1-\delta} = 1+\delta+\delta^2+\ldots$ **thus,**

$$\frac{1}{1-\delta}-\frac{1}{1+\delta} = 2\delta+2\delta^3+\ldots \quad \text{also} \quad \frac{\delta}{1+\delta} = 1-\frac{1}{1+\delta}$$

so that we may, to good approximation, write

$$\frac{d}{ds}\langle x^2\rangle = 2\langle xx'\rangle \qquad \frac{d}{ds}\langle xx'\rangle = \langle x'^2\rangle + K_{xx}\langle x^2\rangle + \frac{K_{xx1}}{2}\left[\left\langle\frac{x^2}{1-\delta}\right\rangle - \left\langle\frac{x^2}{1+\delta}\right\rangle\right] + O\left(x^2\delta^3\right)$$

$$\frac{d}{ds}\langle x'^2\rangle = 2K_{xx}\langle xx'\rangle + K_{xx1}\left[\left\langle\frac{xx'}{1-\delta}\right\rangle - \left\langle\frac{xx'}{1+\delta}\right\rangle\right] + O(xx'\delta^3)$$

$$\frac{d}{ds}\left\langle\frac{xx'}{1+\delta}\right\rangle = \left\langle\frac{x'^2}{1+\delta}\right\rangle + K_{xx}\left\langle\frac{x^2}{1+\delta}\right\rangle - K_{xx1}\left\langle\frac{x^2}{1+\delta}\right\rangle + K_{xx1}\langle x^2\rangle \qquad \frac{d}{ds}\left\langle\frac{x^2}{1+\delta}\right\rangle = 2\left\langle\frac{xx'}{1+\delta}\right\rangle$$

$$\frac{d}{ds}\left\langle\frac{x'^2}{1+\delta}\right\rangle = 2K_{xx}\left\langle\frac{xx'}{1+\delta}\right\rangle + 2K_{xx1}\langle xx'\rangle - 2K_{xx1}\left\langle\frac{xx'}{1+\delta}\right\rangle$$

Truncated set of equations forms closed set.

both methods give nearly identical results for $\langle\delta^2\rangle$ in the regime of interest; similar equations for $\langle x^2/(1-\delta)\rangle$, $\langle xx'/(1-\delta)\rangle$, $\langle x'^2/(1-\delta)\rangle$, and the same set for y; 18 equations total.

Comparison of moment equations with Particle-in-Cell (WARP[1]) simulations (1% velocity spread)

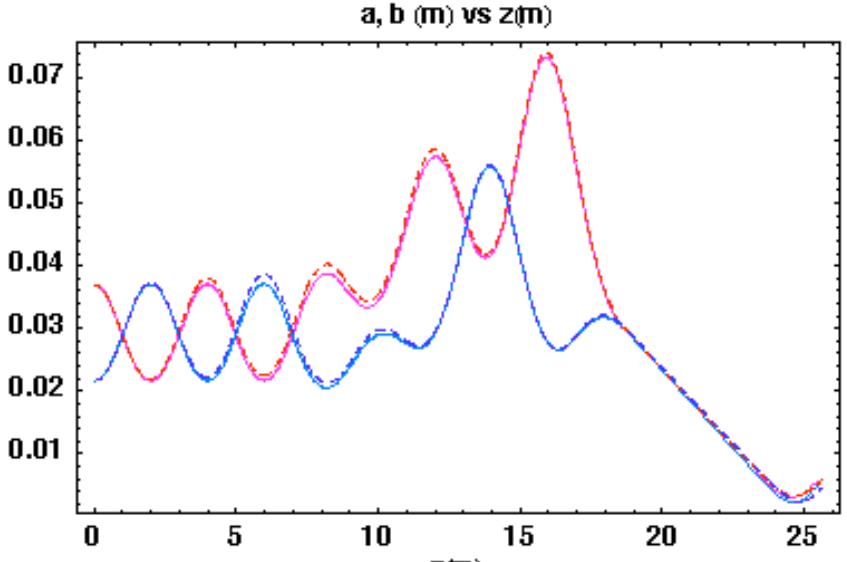

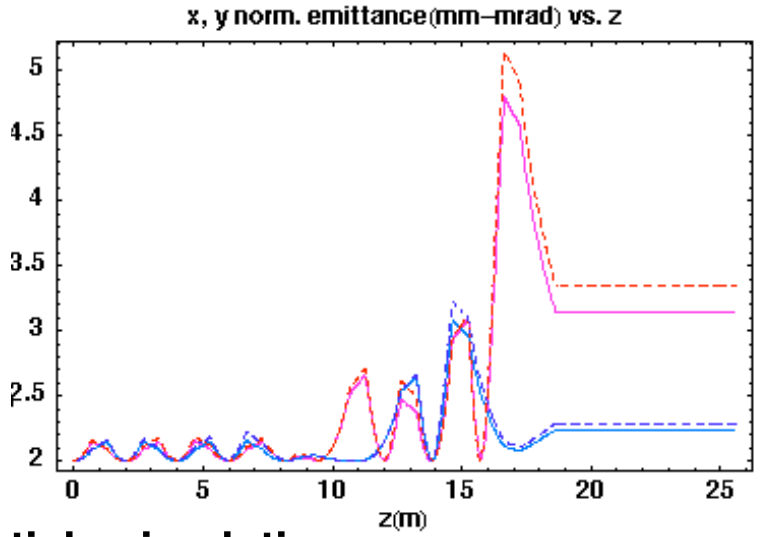

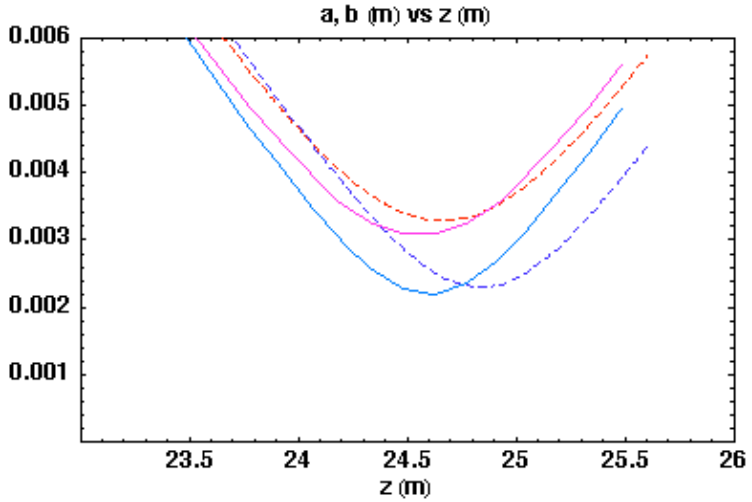

Particle simulations:
Dashed, red (x) and blue (y)
Initial distribution: KV

Moment calcluations:
Solid, magenta (x), and aqua (y)

Result: $\varepsilon_{xc} \cong \alpha_{cx} d\left(\frac{\delta p}{p}\right)\theta_x^2$

α_{cx}**= 4 -12 depending on geometry and initial** $\langle x\delta p\rangle$

Comparison of moment equations with PIC simulations (WARP) -- no velocity spread

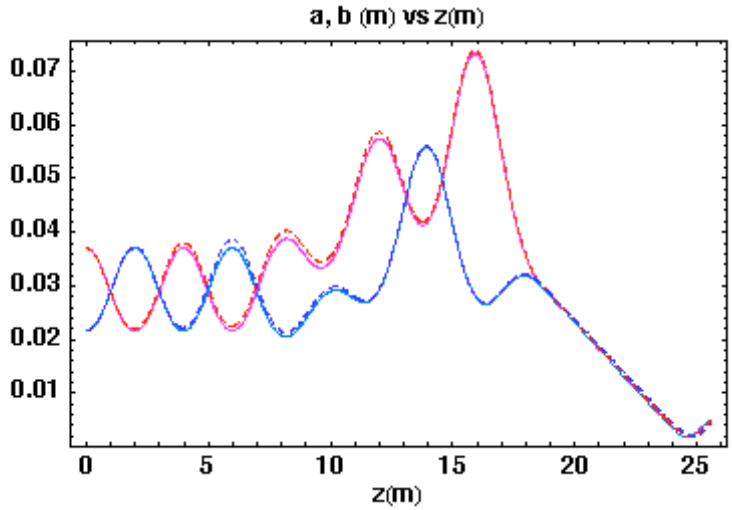

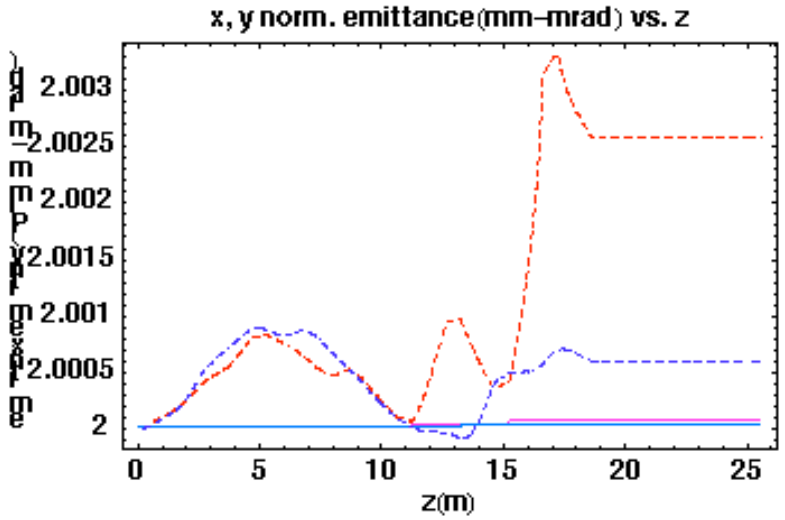

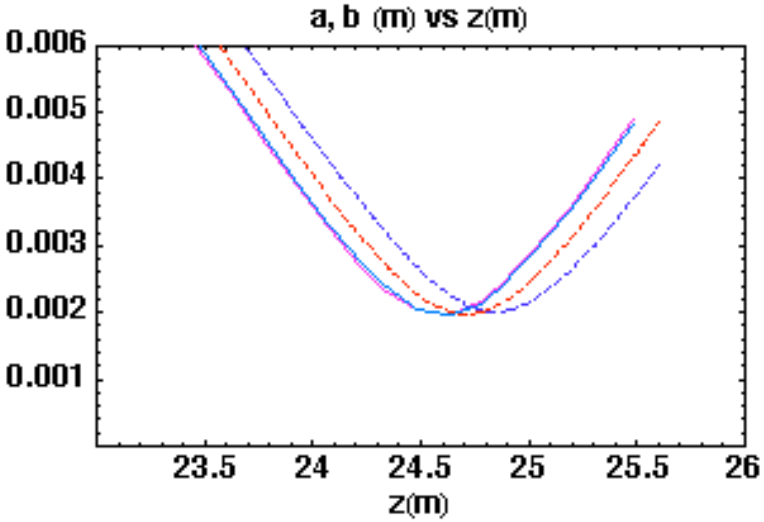

Particle simulations:
Dashed, red (x) and blue (y)
Initial distribution: KV
Moment calcluations:
Solid, magenta (x), and aqua (y)

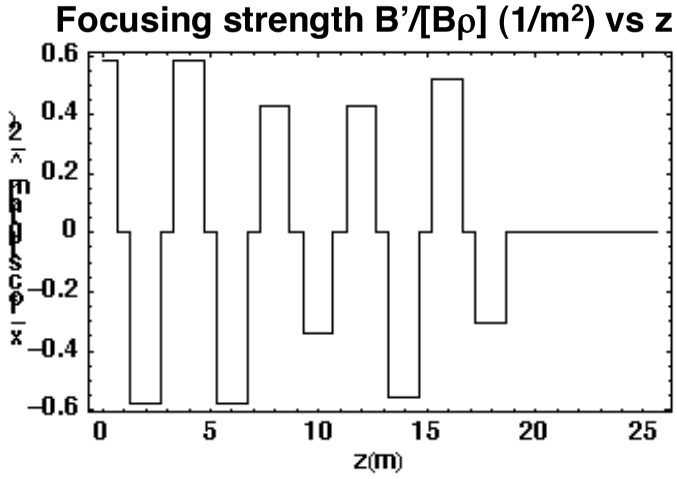

HIF related research has been carried out at LBNL on NDCX-II

Goal: ~30 nC Li^+, 1.2 MeV, or ~70 nC He^+
Beam radius ~ 0.6 mm
Beam pulse duration ~ 1 ns

Goal is to heat solid targets to kT ~ 1 eV before expansion cools target material. This is in the "Warm Dense Matter" (WDM) regime, where material properties are poorly known. Temperature, velocity, and density measurement will constrain Equation of State, conductivities and other properties in the WDM regime.

After the beam of NDCX-II (Neutralized Drift Compression Experiment II) is accelerated plasma is injected into the beam line to eliminate space charge effects in drift compression and final focus

HIF/WDM beam science: neutralized focusing and neutralized drift compression are being tested now for use in WDM and HIF applications

Both techniques minimize the effects of space charge on transverse and longitudinal compression

Transverse compression: vapor from liquid walls in HIF chamber would strip beam, so neutralization required to focus beam in liquid walled chamber. Recent VNL experiments, eg. scaled final focus experiment, (MacLaren et al 2002), NTX (Roy et al 2004), and current NDCX-1 have demonstrated benefits of neutralization by plasmas

Longitudinal compression: WDM experiments require very short, intense pulses (<~ 1 ns) (shorter durations than required by HIF). Neutralization allows what would be very high perveance beams in absence of neutralization (~ 10^{-2}). Modular HIF concept also pushes limits of high perveance beams (since ions have lower accumulated voltage to minimize accelerator length).

NDCX-II has 27 cells (12 powered), a neutralized drift section, a final focus lens, and a target chamber

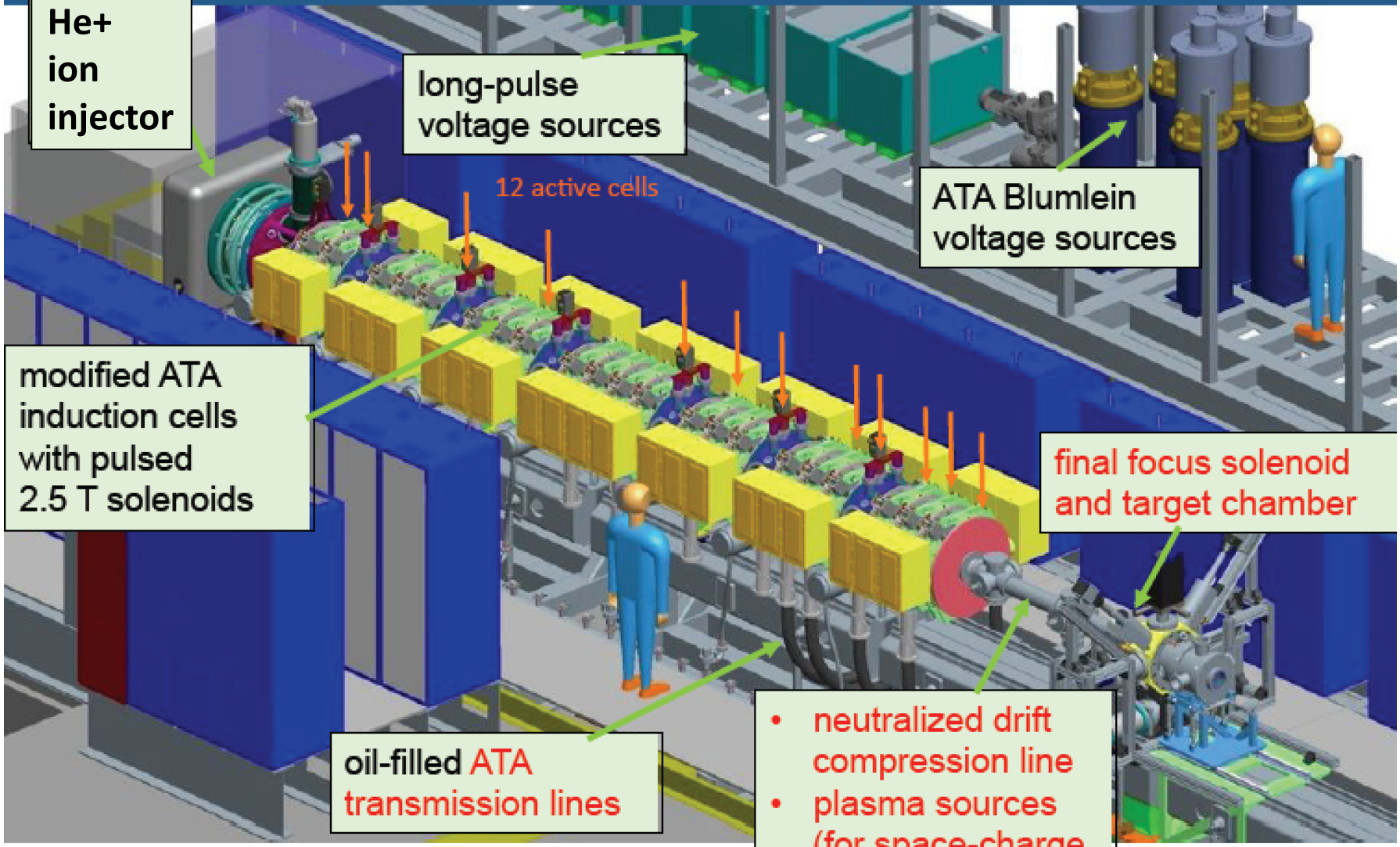

The Particle-in-Cell code WARP was used to help design the machine (see movie)

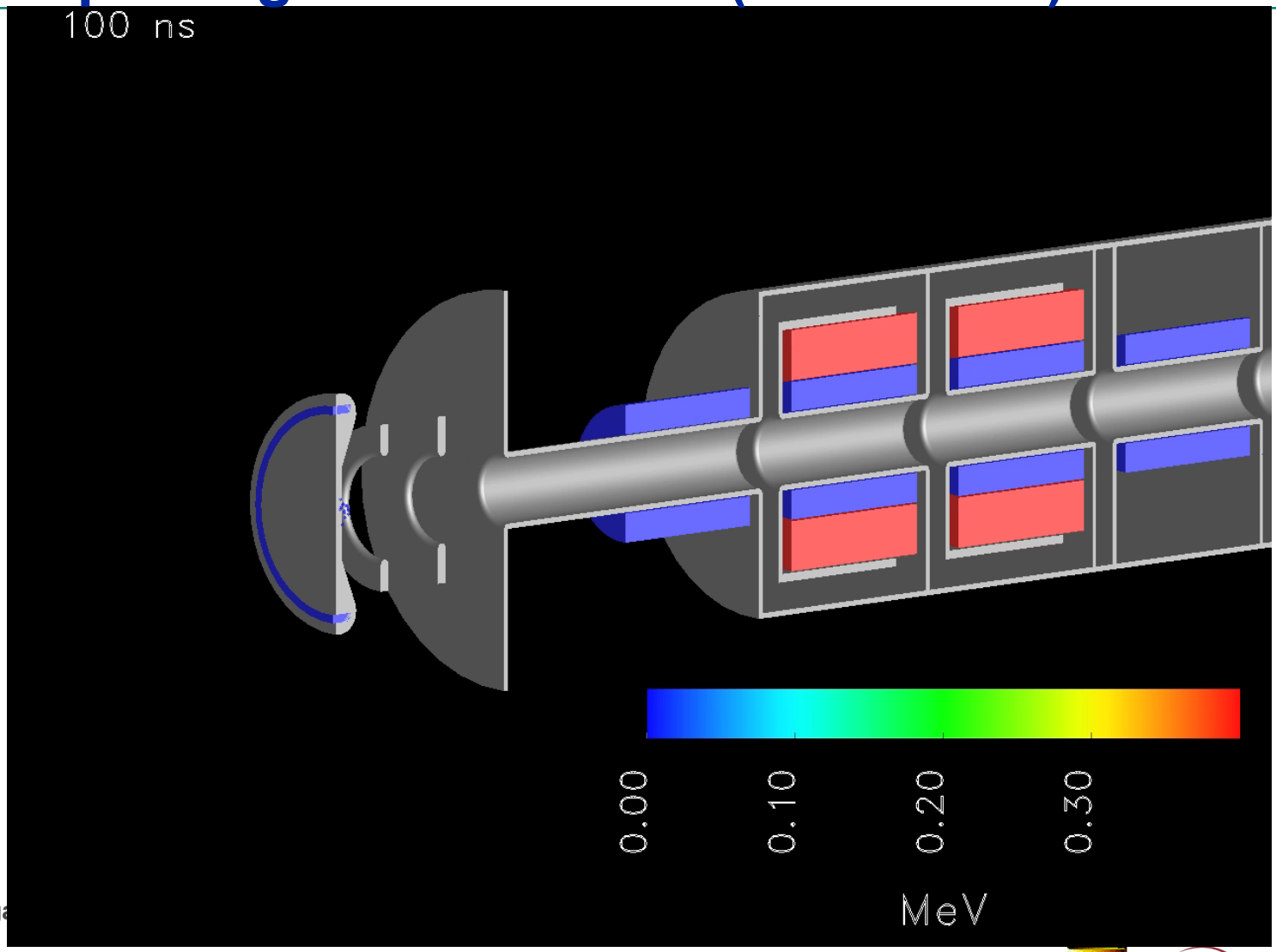

WARP simulation by Dave Grote and Alex Friedman

Artist's conception of HIF Power Plant on a few km^2 site